


Deletion of the transcription factors Hsf1, Msn2 and Msn4 in yeast uncovers transcriptional reprogramming in response to proteotoxic stress

Moritz Mühlhofer¹, Felix Offensperger², Sarah Reschke³, Georg Wallmann², Gergely Csaba², Evi Berchtold², Maximilian Riedl¹, Helmut Blum³, Martin Haslbeck¹, Ralf Zimmer² and Johannes Buchner¹ 

1 Center for Protein Assemblies, Department of Bioscience, Technische Universität München, Garching, Germany

2 Institute of Bioinformatics, Department of Informatics, Ludwig-Maximilians-Universität München, München, Germany

3 Laboratory for Functional Genome Analysis at the Gene Center, LMU München, München, Germany

Correspondence

J. Buchner, Center for Protein Assemblies, Department of Chemistry, Technische Universität München, Ernst-Otto-Fischer Strasse 8, Garching 85747, Germany
Tel: +498928913340
E-mail: johannes.buchner@tum.de

(Received 19 December 2023, revised 15 January 2024, accepted 18 January 2024, available online 16 February 2024)

doi:10.1002/1873-3468.14821

Edited by Hitoshi Nakatogawa

The response to proteotoxic stresses such as heat shock allows organisms to maintain protein homeostasis under changing environmental conditions. We asked what happens if an organism can no longer react to cytosolic proteotoxic stress. To test this, we deleted or depleted, either individually or in combination, the stress-responsive transcription factors Msn2, Msn4, and Hsf1 in *Saccharomyces cerevisiae*. Our study reveals a combination of survival strategies, which together protect essential proteins. Msn2 and 4 broadly reprogram transcription, triggering the response to oxidative stress, as well as biosynthesis of the protective sugar trehalose and glycolytic enzymes, while Hsf1 mainly induces the synthesis of molecular chaperones and reverses the transcriptional response upon prolonged mild heat stress (adaptation).

Keywords: heat shock response; Hsf1; Msn2/4; transcriptome; proteome; proteostasis

Life depends on the ability to respond to adverse changes in the environment such as unphysiologically high temperatures [1,2]. As different proteotoxic stresses lead to the accumulation of unfolded proteins and a stop in translation and growth, these stresses can be counteracted by a shared transcriptional program, the heat shock response (HSR) [1,2]. This was already indicated much earlier by observations of thermotolerance in which exposure to one stress protects cells against another stress [3,4]. To counteract proteotoxic insults, a specific set of stress-protective proteins, called heat shock proteins is upregulated under stress [1,2,5,6]. Those proteins help to maintain proteostasis

by preventing or even reversing the aggregation of unfolded proteins [7,8]. The transcriptional response comprises several hundred genes that are changed in their expression at least two-fold in comparison to the non-stress situation [9,10]. Recently, we showed that the reprogramming induced by mild heat stress was only transient and that yeast is able to adapt to mild heat stress. In addition, many non-chaperone genes seemed to be upregulated to counteract the increased protein turnover under stress and hence to guarantee constant protein levels [10]. Heat shock factors (HSFs) are generally thought to be the regulators of the HSR in eukaryotes [11–13]. The main regulators

Abbreviations

CWI, cell wall integrity pathway; ESR, environmental stress response; GO, gene ontology; HSR, heat shock response; ISR, integrated stress response; KO, knock-out; LFQ-MS, label-free quantification mass spectroscopy; TF, transcription factor; UPR, unfolded protein response; WT, wild-type.

of the transcriptional HSR in yeast are Hsf1, Msn2, and Msn4 [14]. Whereas vertebrates usually express several HSFs, yeast only encodes Hsf1, which is an essential protein [15–17]. Interestingly, only 18 Hsf1-dependent genes (HDGs) were identified in *Saccharomyces cerevisiae* and the essential function of Hsf1 could be further narrowed down to the regulation of Hsp70 and Hsp90 expression under physiological conditions [18].

Further important regulators of the response against proteotoxic insults in yeast are the two highly homologous transcription factors (TFs) Msn2 and Msn4 [19–22]. As they can be activated by various stresses [14], they are not only linked to the HSR but more generally associated with the environmental stress response [21–27]. The several hundred genes targeted by Msn2 and Msn4 are partially redundant but for a full transcriptional activation of most of their targets both TFs seem to be necessary [22,28]. Furthermore, there is an overlap of several chaperone encoding genes that are regulated by Hsf1 and Msn2/4 [29].

While we have reached a profound understanding of the stress response, there is a central open question: what happens to an organism in the complete absence of a stress response. Addressing this question would reveal the stress-sensitive segment of the proteome and it would allow identifying the detrimental effects of stress on cells. To approximate this, a yeast strain was created which combines the conditional nuclear depletion of Hsf1 [18,30] with the deletion of the *MSN2* and *MSN4* genes. The analysis of the transcriptional response of cells lacking either Hsf1, Msn2/Msn4 or all three transcription factors to mild (37 °C) and severe (42 °C) heat stress revealed their individual contributions as well as the consequence of a total loss of this core stress response. This allowed the analysis of the part of the proteome which is protected by the Hsf1 and Msn2/4 targets. Furthermore, sporulation induced *via* the cell wall integrity pathway was identified as a potential survival strategy in the complete absence of the stress response.

Materials and methods

Yeast cultivation and heat shock experiments

W303 yeast cells were grown in YPD-A (100 mg·L⁻¹ adenine) at 25 °C from an OD₅₉₅ of 0.3 to an OD of 0.8 while shaking. Then, the cells (50 mL) were shifted to 37 or 42 °C (water bath), respectively for up to 60 min. The control cells were kept at 25 °C. After the heat shock, the cells were harvested for 1 min at 4000 *g* at 4 °C.

Genomic deletion of *MSN2* and *MSN4*

MSN2 and *MSN4* genes were deleted by homologous recombination with transformed linear knock-out cassettes [31]. PCRs were performed as described previously [31] using the following primers: *MSN2* fw: TCTTTCTTTTTTCAACTTT-TATTG CTCATAGAAGAACTAGATCTAAAATGCG-TACGCTGCAGGTCGAC; *MSN2* rev: AATTATC TT ATGAAGAAAGATCTATCGAATTAATAAATGGGG TCTATTAATCGATGAATTCGAGCTCG; *MSN4* fw: TTATCAGTTCGGCTTTTTTTTTCTTTTCTTCTTATT AAAACAATATAATGC GTACGCTGCAGGTCGAC; *MSN4* rev: AATTATCTTATGAAGAAAGATCTATCGAATTAATAA AAATGGGGTCTATTAATCGATGAA TTCGAGCTCG. The purified PCR products were transformed into mid-logarithmic yeast cells (OD₅₉₅ of 0.6–0.8). After harvesting the cells (5 min at 3000 *g*), they were washed with 25 mL water. Then, the cells were resuspended in 1 mL 0.1 M lithium acetate. 50 µL of the cell suspension were used for the transformation and again pelleted. The cells were resuspended in 240 µL PEG (50% w/v), 36 µL 1 M lithium acetate, 6 µL ssDNA and 0.1–10 µg DNA. The suspension was filled to 360 µL with water, vortexed, incubated for 30 min at 30 °C and subsequently for 30 min at 42 °C. To remove the transformation mixture, the cells were spun down for 15 s at 5200 *g* and 1 mL of warm YPD/CSM was added to allow the cells recover for 1–2 h. 200 µL were plated on selection media and incubated at 30 °C for 2–4 days. To select for correct positive clones, the colonies were transferred onto replica plates with the same selection marker after 3 days. Genomic insertion was checked with colony PCR.

Spot assays

Yeast overnight cultures were diluted to an OD₅₉₅ of 1 in YPD-A and 5 µL spotted on an YPD-A agar plate. The cells were incubated for 24 h on a temperature gradient plate (29–48 °C; Biometra, Jena, Germany).

Nuclear depletion of Hsf1

For the depletion of Hsf1, genetically engineered yeast cells [18] were grown to an OD₅₉₅ of 0.6–0.7 and then treated with 1 µM rapamycin (solved in DMSO). The control cells were treated with an equal volume of DMSO. After the addition of rapamycin, the cells were incubated for 45 min at 25 °C and then the heat stress was performed as described above.

Live/dead staining

To check cell survival after prolonged nuclear depletion of Hsf1, live/dead staining was performed using Trypan blue. Cells were harvested by centrifugation at 3000 *g* for 1 min.

The pellet was resuspended in 1 mL PBS containing a final concentration of $10 \mu\text{g}\cdot\text{mL}^{-1}$ Trypan blue. Cells were counted discerning between unstained living cells and blue-stained dead cells [32]. Cells that had taken up the dye were classified as dead [33].

RNA isolation

RNA isolation was performed based on a published protocol [34] with a few adjustments. In brief, 3×10^6 cells were harvested (9000 *g* for 1 min at 4 °C) and the pellets were shock frozen in liquid nitrogen. The cell pellets were resuspended in 400 μL TES buffer (10 mM Tris/HCl, pH 7.5, 10 mM EDTA, 0.5% SDS) and 400 μL acidic phenol were added. The suspension was incubated for 30 min at 65 °C while shaking (900 r.p.m.). After 5 min on ice, the suspension was centrifuged for 5 min at 25 000 *g* and 4 °C. The aqueous phase was transferred into a fresh 1.5 mL tube, further 400 μL acidic phenol were added and the procedure was repeated. After the aqueous phase was again transferred into a fresh tube, 400 μL of chloroform were added, it was vortexed and centrifuged for 5 min at 25 000 *g* and 4 °C. The aqueous phase was once more transferred into a fresh tube and the RNA precipitated by the addition of 40 μL 3 M sodium acetate (pH 5.3) and 1 mL ice-cold ethanol. The RNA was pelleted for 60 min at 25 000 *g* and 22 °C and the supernatant was discarded. The pellet was washed two times with 1 mL 70% ice-cold ethanol. Finally, the dried RNA pellets were dissolved in 20 μL RNase-free water and incubated for 20 min at 37 °C while shaking (900 r.p.m.). The concentration was measured on a Nanodrop spectrometer (Thermo Fisher Scientific, Waltham, MA, USA) and the quality of the RNA samples checked on an Agilent Bioanalyzer (RNA 6000 Nano kit; Agilent, Santa Clara, CA, USA).

Preparation of RNA libraries and RNA sequencing

Libraries were generated with the help of the Lexogen SENSE mRNA-seq Library Prep Kit V2 (Lexogen GmbH, Vienna, Austria) with half of the volume as described in the manual. First, the magnetic beads were washed two times with the provided buffer. After thermal denaturation of the RNA for 1 min at 60 °C, 500 ng RNA were added to the beads in hybridization buffer. After hybridization of the RNA (20 min at RT and 1250 r.p.m.), the beads were washed again twice with 50 μL of the provided wash buffer. After removing the supernatant, 7.5 μL of the provided reverse transcription and ligation mix as well as 1 μL Starter/Stopper mix were added and mixed by vortexing. The reverse transcription reaction was incubated for 5 min at 25 °C and 1250 r.p.m., then 1.5 μL of enzyme mix 1 were added to ligate the reverse transcribed cDNA fragments. It was vortexed again and incubated for additional 2 min at 25 °C and 1250 r.p.m. Subsequently, the samples were incubated for 1 h at 37 °C and 1250 r.p.m. To stop the reaction,

50 μL wash buffer were added. The beads were washed with 50 μL wash buffer once more and then they were resuspended in 8.5 μL second strand synthesis mix. At this point, 0.5 μL of the provided enzyme mix 2 was added. The second strand was synthesized with the following program in a PCR cyclor: 1 cycle: 90 s at 98 °C, 60 s at 65 °C, 5 min at 72 °C, hold at 25 °C. The samples were purified as described in the provided user manual. Finally, the cDNA samples were eluted with 8.5 μL of the provided elution buffer. For the library amplification, 3.5 μL of the provided PCR mix and 0.5 μL enzyme mix 2 per reaction were added to the eluted library. 2.5 μL i7 primers were added and 9 cycles of PCR with the following program were run: 98 °C for 10 s, 65 °C for 20 s, 72 °C for 30 s and a final extension at 72 °C for 1 min (hold at 10 °C). The PCR products were purified with Agencourt AMPure XP beads (Beckman Coulter, Brea, CA, USA). 36 μL of purification beads were used. The quality of the libraries was checked with an Agilent Bioanalyzer (DNA 1000 Kit).

Next-generation sequencing

DNA libraries were sequenced on a HiSeq1500 sequencer (Illumina, San Diego, California, USA) with 200–240 million reads per lane. RNA-seq experiments were sequenced with 10 million 50 bp single end reads. A total of 570×10^6 sequences were generated.

Soluble/insoluble fractionation

Cell lysis and soluble/insoluble fractionation were performed as described elsewhere [10,35]. The pellets (50 mL culture) were washed once in 1 mL ice-cold buffer S₀ (20 mM HEPES/KOH, pH 7.4, 120 mM KCl, 2 mM EDTA; 30 s at 5000 *g* and 4 °C) and frozen in 2 mL Eppendorf tubes in liquid nitrogen. To lyse the cells, the thawed pellets were resuspended in 150 μL buffer S (20 mM HEPES/KOH, pH 7.4, 120 mM KCl, 2 mM EDTA, 0.5 mM DTT, 1 : 100 protease inhibitor MixFY (SERVA Electrophoresis GmbH, Heidelberg, Germany), 1 mM PMSF). Half of the cell suspension was also flash-frozen in liquid nitrogen and lysed in a mixer mill (Retsch GmbH, Haan, Germany) with 9 mm stainless steel balls (4 × 90 s at 30 Hz; Cole-Parmer, Vernon Hills, IL, USA) that were prechilled in liquid nitrogen. The tubes were cooled in liquid nitrogen between the cycles. Before the lysate was cleared for 30 s at 3000 *g* and 4 °C, 400 μL ice-cold buffer S were added. The cleared supernatant was then transferred into a 1.5 mL ultracentrifuge tube (Beckman Coulter) and the insoluble fraction was separated from the soluble fraction by ultracentrifugation for 25 min at 114 480 *g* (TLA-45) and 4 °C (Optima Max E Ultracentrifuge; Beckman Coulter). The soluble fraction was transferred into a fresh, precooled tube (S) and the pellet was washed once with 500 μL buffer S (41 000 r.p.m. for 25 min at 4 °C). The remaining pellet

was dissolved in 500 μL buffer P (8 M urea, 20 mM HEPES/NaOH, pH 7.4, 150 mM KCl, 2 mM EDTA, 2% (m/v) SDS, 2 mM DTT, 1 : 1000 protease inhibitor MixFY (SERVA), 10 μM PMSF) by vigorous vortexing in a thermal shaker for 30 min at RT. Finally, this solution was spun down for 5 min at 20 000 *g* and RT and the aqueous phase was taken as the pellet (P) fraction. The concentration of the samples was determined *via* BCA assay (ThermoFisher Scientific, Waltham, MA, USA).

Sample preparation for MS/MS measurements

250 μg protein were precipitated to get rid of detergents and inhibitors [36]. First, the volume of the protein sample was adjusted to 160 μL with H_2O in Eppendorf tubes. 600 μL methanol (Sigma-Aldrich, St. Louis, MO, USA) were added and the emulsion was vortexed and centrifuged for 10 s at 16 200 *g* and RT. This procedure was repeated with 225 μL chloroform (Sigma-Aldrich). Then 450 μL H_2O were added, it was vortexed again, incubated for 7 min in an ultrasonic bath (VWR, Radnor, Pennsylvania, USA) and centrifuged for 10 s at 16 200 *g*. The upper phase was taken off until the precipitated proteins in the interphase were reached. After the addition of 450 μL methanol, the suspension was vortexed and centrifuged at 16 200 *g* for 20 min at RT. The supernatant was discarded and the pellets were air-dried. The proteins were dissolved in 8 M urea, 50 mM Tris (pH 7.5), 4 mM DTT. 20 μg protein were transferred into a fresh Eppendorf tube and diluted with 50 mM Tris to a final volume of 25 μL (2 M Urea, 50 mM Tris pH 7.5, 1 mM DTT). Subsequently, the proteins were digested with sequencing grade Trypsin (5 $\text{ng}\cdot\mu\text{L}^{-1}$; Promega, Madison, WI, USA) for 2 h at RT. The peptides were alkylated (50 mM Tris/HCl, pH 7.5, 2 M urea, 5 mM IAA) in the dark at RT overnight at 500 r.p.m. in a thermomixer. Then, the tryptic digest was quenched with 1.5 μL formic acid (FA). The samples were desalted with double C18 layer stage tips [37]. To this end, the tips were equilibrated with 70 μL methanol and washed three times with 70 μL 0.5% FA by applying mild centrifugation steps (960 *g*). The peptides were loaded onto the tips, washed three times with 70 μL 0.5% FA and eluted with two times 30 μL 80% ACN, 0.5% FA (960 *g*). The samples were dried in a speed vacuum concentrator (Eppendorf, Hamburg, Germany). For the MS/MS measurement, the peptides were dissolved in 23 μL 1% (v/v) FA and incubated for 15 min in an ultrasonic bath at RT. The peptide solutions were filtered with centrifugal filters (0.22 μm ; Merck, Darmstadt, Germany; 1 min at 7000 *g*) and transferred into Chromacol vials (ThermoFisher Scientific).

MS/MS measurements

MS/MS measurements were performed on an Orbitrap Fusion coupled to an Ultimate3000 Nano-HPLC *via* an electrospray source (all ThermoFisher Scientific). After

loading the peptides on a 2 cm PepMap RSLC C18 trap column (particles 3 μm , 100 \AA , inner diameter 75 μm , ThermoFisher Scientific) with 0.1% TFA, they were separated on a 50 cm PepMap RSLC C18 column (particles 2 μm , 100 \AA , inner diameter 75 μm , ThermoFisher Scientific) constantly held at 40 $^{\circ}\text{C}$. The peptides were eluted with a gradient from 5% to 32% ACN, 0.1% FA during 152 min at a flow rate of 0.3 $\mu\text{L}\cdot\text{min}^{-1}$ (7 min 5% ACN, 105 min to 22% ACN, 10 min to 32% ACN, 10 min to 90% ACN, 10 min wash at 90% ACN, 10 min equilibration at 5% ACN). Survey scans (m/z 300–1500) with a resolution of 120 000 were acquired. The automatic gain control (AGC) target value was set to $2.0\cdot 10^5$ with a maximum injection time of 50 ms. For fragmentation with high-energy collisional dissociation, the most intense ions of charge states 2–7 were selected. The collision energy was set to 30%. In the ion trap, the maximum injection time was also set to 50 ms and the AGC target value was reduced to $1.0\cdot 10^4$. Inject ions for all available parallelizable time was allowed. Dynamic exclusion of sequenced peptides was set to 60 s. Internally generated fluoroanthene ions were used for real-time mass calibration. Data were acquired using XCALIBUR software version 3.0sp2 (ThermoFisher Scientific).

MS/MS data analysis

The MS data were analyzed with MAXQUANT (version 1.6.2.6) [38,39]. The reviewed *S. cerevisiae* proteome database downloaded from UniprotDB (2018) was used for protein identification. The same fraction was set for all files of one experimental setup. Only tryptic peptides were searched and cleavage sites before proline were included. Peptides with up to two missed cleavage sites were included in the analysis and a peptide tolerance of 4.5 ppm was applied. N-terminal acetylation and methionine oxidation were selected as variable modifications. As fixed modification, carbamidomethylation was selected. Not more than five modifications per peptide were allowed. For the primary search in MAXQUANT the min. ratio count was set to 1 and Label min. ratio count was also set to 1. Furthermore, unique + razor peptides were taken into account. Otherwise, the preset orbitrap instrument settings of MAXQUANT were applied. The minimal peptide length was set to seven amino acids, the maximal length was 25 amino acids. Match between runs was applied (match time window: 0.7 min; align window: 20 min). The identification parameters were left preset with a protein false discovery rate (FDR) of 1%. The peptides were also searched against a decoy database (reverse database) generated by MaxQuant. The protein groups table that was generated by MAXQUANT was further evaluated in PERSEUS (version 1.6.2.1) [40]. First, the table was filtered by potential contaminant hits, hits from the reverse (decoy) database and hits that were only identified by side. After \log_2 transformation of the LFQ intensities, the associated replicates were grouped into

categories. Then, the rows were filtered on three valid values in at least one group. The missing values were calculated from the Gaussian distribution (width: 0.3; downshift: 1.8). To analyze the fold changes, Volcano plots were plotted and a two-sided *t*-test was applied [41] in PERSEUS. A protein was considered to be significantly up- or downregulated if $|\log_2 \text{fc}| > 1$ and *P*-value < 5%.

Processing of RNA-seq datasets

The quality-controlled sequencing reads were aligned to the yeast reference genome (yeast genome 2011; R64-1-1 (ENSEMBL version 75)) [42] using the mapping tool CONTEXTMAP2 (v.2.8.0) [43]. CONTEXTMAP2 tries to resolve ambiguous i.e. multi-mapped reads by a simple context-based approach assigning reads to the most plausible positions based on the mapping of the other reads. Gene quantification was performed using FEATURECOUNTS (v.2.0.0) [44] at the gene level to the corresponding yeast gene transfer format. Hereby a minimum fraction of 0.5 of overlapping bases were required for assigning a read to a feature and only primary alignments were considered. These gene counts were normalized and further analyzed by DESEQ2 (v.1.28.1) [45] for pairwise differential expression analysis. Knock-out and wild-type strains were always compared to the 25 °C reference of the same strain, thereby eliminating bias of the knock-out as best as possible. These pairwise fold changes are the basis for subsequent multidimensional analysis of the dataset.

Principal component analysis (PCA)

To get a first overview over the transcriptomic changes taking place, a PCA was applied to the preprocessed normalized gene counts [46]. The PCA finds a projection of the samples in few (typically two are visualized) dimensions such that the samples are arranged according to components displaying the largest overall variance among the samples. Dimensionality reduction methods were accessed *via* the SKLEARN (v.0.0) module [47] in PYTHON (v.3.6.13), without any filtering of the genes before reduction. The individual conditions were visually represented in groups and the centroids of the three samples per condition were linked to each other by directional arrows corresponding to the time points.

Sankey plots

Fold changes from DESEQ were categorized into ‘linguistic’ classes. Depending on how strong the regulation was, fold changes above 1 were considered as slightly differentially expressed (‘up’, ‘down’) and above 2 as strongly differentially expressed (‘strong up’, ‘strong down’), resulting in five classes. Genes for which no significant change could be detected were classified as ‘unchanged/no assumption’.

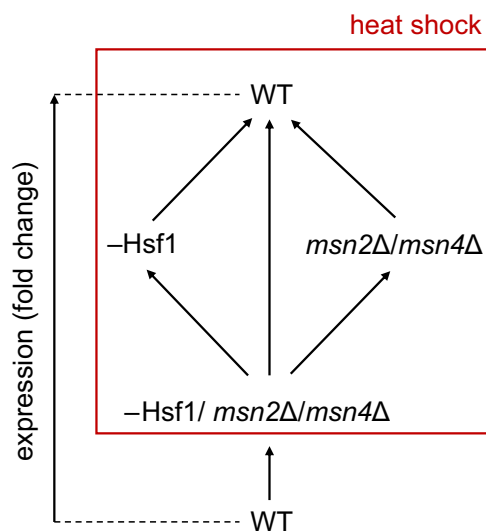
Sankey diagrams (PLOTLY v.4.9.3) [48] were plotted to show the fluxes of genes in/out the respective class along certain selected dimensions, e. g. the time after the heat shock.

Expression component analysis (ECA)

As another method to dissect high dimensional transcriptomic data, expression component analysis (ECA) was applied [49]. ECA tries to extract the effect of the absence of transcription factors (TF) on each individual gene in a systematic manner by taken into account individual knock-outs/–downs of two TFs together with the respective combination of both TFs. This allows to reduce the data from the different knock-out and depletion strains to produce effect models for each gene.

The ECA is based on the assumption that the fold change difference between two transcriptomic states is the result of the presence or absence of transcription factors. All transcription factors, Hsf1 and Msn2/4, can thereby contribute to the abundance of transcripts. For the three transcription factors, in total four different transcriptomic states (WT, *msn2Δ/msn4Δ*, Hsf1 depletion (–*Hsf1*), and *msn2Δ/msn4Δ* + Hsf1 depletion (–*Hsf1/msn2Δ/msn4Δ*) were measured in triplicates).

Between these four states, the fold changes between five transitions are of interest (see Scheme 1). In these transitions either one or two of the TFs are added and, thereby give rise to a fold change of the transcript abundance. This interaction is modeled by a linear combination of three expression components. First, a component ‘H’ is dependent on the rapamycin based Hsf1 depletion and an ‘M’ component is dependent on the Msn2/4 knock-out. Second,



Scheme 1. Schematic representation of the conducted expression component analysis (ECA).

a third cooperative component 'Co' is added. This component accounts for possible regulatory interactions between the two transcription factors and for redundant or synergistic effects.

These three components are calculated by fitting the linear ECA model to the pairwise fold changes between the measured transcript abundancies. All possible combinations of the three biological replicates for each strain are considered which allows to assess the significance of the resulting effect strengths.

Quantification and statistical analysis

Statistical parameters are reported in the figures and figure legends. Statistical significance was assigned by using a two-sample *t*-test. *P*-values below 0.05 were considered significant. Genes or proteins that exhibited at least a two-fold change under stress compared to the unstressed condition were defined to be differentially expressed. Statistical analyses were performed using PERSEUS, ORIGIN and R. For specific methods, the respective software used is mentioned in the associated methods.

Results

Stress-protective transcription factors regulate the transcription of several genes under non-stress conditions

To analyze the HSR in yeast in the absence of a protective system, we depleted the essential TF Hsf1 from the nucleus (*-Hsf1*) via the 'Anchor-Away system' as described previously [18,30] (Fig. 1A). To this end, Hsf1 was fused to the FRB (FKBP12 rapamycin binding) domain and the ribosomal subunit RPL13A was fused to FKBP12 [18]. Furthermore, the yeast strain carried a *TOR1* mutation to make it resistant to rapamycin [30]. Conditional depletion was achieved by the addition of rapamycin to the cells, which induced the dimerization of FRB and FKBP12 and the subsequent nuclear export of Hsf1 together with the ribosomal subunit [18,30]. It was shown before that after 20 min of rapamycin treatment, Hsf1 was efficiently depleted from the nucleus [18]. Additionally, we deleted the stress-specific transcription factors Msn2 and Msn4. First, we tested the thermo-sensitivity of the *msn2Δ/msn4Δ* strain in comparison to the wild-type control strain (WT). The WT exhibited a maximum growth temperature of around 41 °C (Fig. S1A). Of note, deletion of both Msn2 and Msn4 did not lead to an increased thermo-sensitivity, consistent with previous observations after short-term stress exposure [28] (Fig. S1A). At 25 °C, the Msn2/4 knock-out (KO) cells reached almost the same densities as the WT after

overnight incubation (Fig. 1B). The growth of yeast in which nuclear Hsf1 was depleted was unaffected up to 3 h of depletion but the cells stopped to grow overnight (Fig. 1B) [18]. Taken together, these findings show that Msn2/4 are not compulsory at physiological conditions while the essential role of Hsf1 was confirmed.

Mild heat stress of 37 °C resulted in decreased growth of cells lacking nuclear Hsf1 and the cells stopped growth upon prolonged incubation (Fig. 1B). The Msn2/4-deleted cells also grew slower than the WT but continued to proliferate overnight (Fig. 1B). Recovery experiments of the Hsf1-depleted cells at 25 °C (following overnight exposure at 37 °C) showed that after a lag phase of 6 h in medium without rapamycin growth was resumed (Fig. S1B). This result suggests that those cells had only entered a dormant stage and did not die. Live/dead staining of the cells using Trypan blue confirmed that at least 90% of the cells lacking Msn2/4 or nuclear Hsf1 had survived overnight exposure at 37 °C (Fig. S1C).

Next, we were interested in the transcriptomic changes induced by the absence of Msn2/4 and Hsf1. Although no influence on cell viability was observed for the Msn2/4 KO strain, the analysis of the transcriptome under physiological conditions revealed that for 23 genes (*MSN2/4* excluded) the transcription was changed at least two-fold (14 decreased, 9 increased) compared to the transcriptome of WT cells (Fig. 1C, D). Among the genes whose basal transcription strongly relies on Msn2/4, we found Hxk1 and Glk1 which both catalyze the phosphorylation of glucose, the first and an essential step of glycolysis, and trehalose biosynthesis (Fig. 1D). Furthermore, the transcription of *PYK2* which encodes a pyruvate kinase, another key enzyme in glycolysis and *NTH1* which is linked to trehalose metabolism are decreased upon the deletion of Msn2/4. In addition, the mRNA levels of *GPH1* which encodes a glycogen phosphorylase are reduced in the absence of Msn2/4. This indicates that Msn2/4 are involved in regulating the supply of glucose from glycogen for energy generation and also for trehalose biosynthesis. Moreover, a positive regulatory effect of Msn2/4 on the mRNA levels of three enzymes involved in stress tolerance was detected. These are glutamate decarboxylase *GAD1*, an enzyme that converts glutamate to γ -aminobutyric acid and is linked to the oxidative stress response [50], the ceramidase *YPC1*, a gene linked to thermotolerance [51] and the stress-induced nicotinamidase *PNC1*. Pnc1 was shown to extend the replicative lifespan of yeast due to calorie restriction [52]. Therefore, its lower transcription rate might positively affect the metabolic turnover and

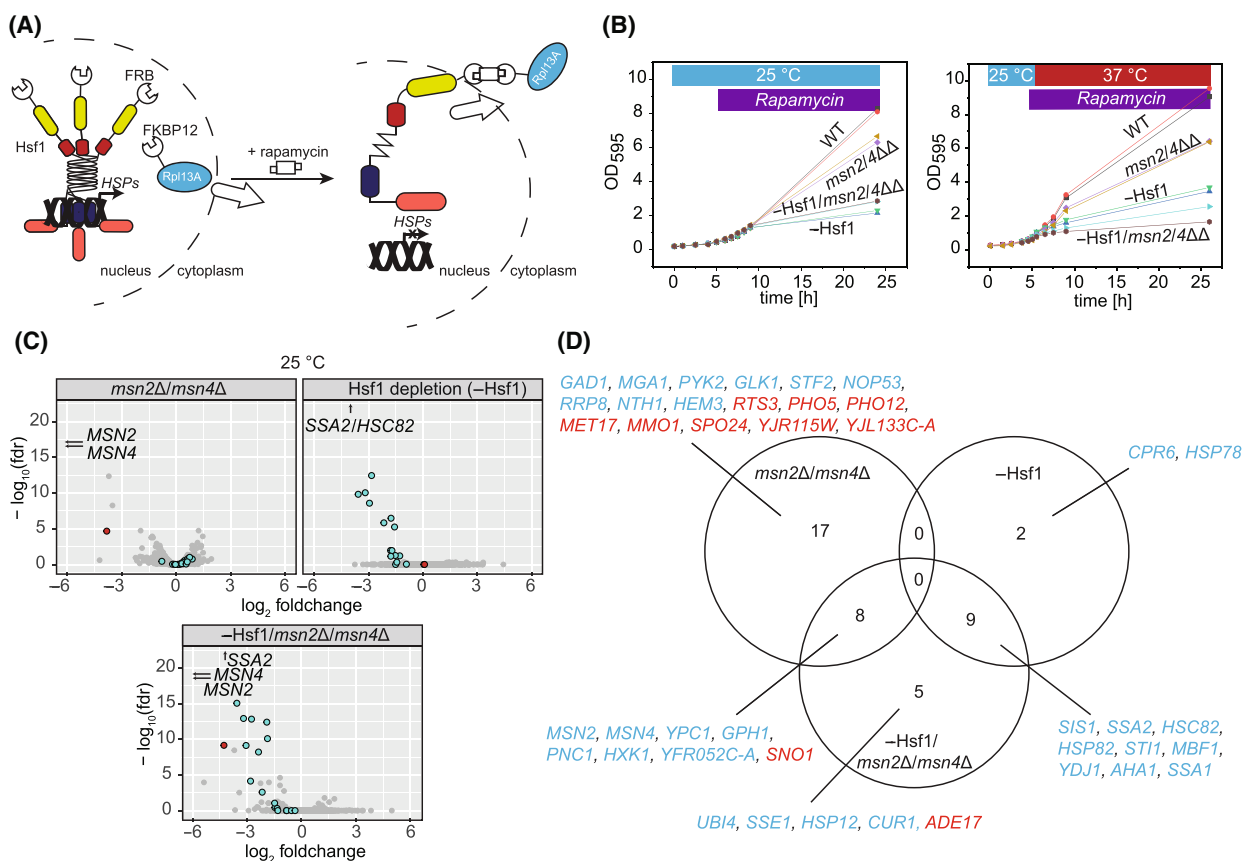


Fig. 1. Depletion of Hsf1 leads to a stop of growth after several hours. (A) Scheme of the general setup of the Hsf1 anchor away system. The FRB domain is fused to the transcription factor and the FKBP12 domain to a ribosomal subunit (Rpl13A). Upon the addition of 1 μM rapamycin, the FRB and FKBP12 domains form dimers and Hsf1 is exported together with the ribosomal subunit from the nucleus. (B) Yeast cells were grown to an OD₅₉₅ of ca. 0.5 at 25 °C. After the addition of 1 μM rapamycin the cells were incubated for 45 min at 25 °C before they were shifted to 37 °C (right panel). The growth measurement was performed in biological duplicates. WT: Black squares and red dots; *msn2Δ/msn4Δ*: beige triangle (pointing left) and purple diamonds; *-Hsf1*: green triangle (pointing down) and blue triangle (pointing up); *-Hsf1/msn2Δ/msn4Δ*: brown circle and cyan triangle (pointing right). Growth after recovery and the viability of stressed cells are shown in Fig. S1B,C. (C) Fold changes and significance values (*P*-values) derived from DESeq for each gene are shown for the basal effect for each knock-out/down strain at 25 °C compared with the WT in volcano plots. The 18 HSF1-dependent genes [18] are colored in blue and *HXK1*, the main glycolytic agent, is colored in red. (D) Venn diagram showing the overlap of transcripts with assigned gene names whose basal transcription was affected at 25 °C by the absence of Msn2/4 and/or Hsf1. Genes with reduced mRNA levels compared to the WT are colored in blue, genes with increased levels in red. Fold changes and significance values (*P*-values) are shown in the volcano plots in (C).

in turn negatively affect the replicative lifespan of the *msn2Δ/msn4Δ* strain. Furthermore, the transcription of a protective gene against desiccation (*STF2*) was decreased whereas the basal mRNA levels of *RTS3*, a putative subunit of the phosphatase PP2A, which is known to activate Msn2 [53], were increased in the absence of Msn2/4 (Fig. 1C,D). The transcription of two of three repressible acid phosphatases (*PHO5* and *PHO12*), which, to our knowledge, have not been linked to the regulation of Msn2 and Msn4 were also increased in *msn2Δ/msn4Δ*. Of note, in the absence of Msn2/4, already at the level of basal transcription an

upregulation of sporulation was indicated (*SPO24*). Furthermore, the transcription of three unknown genes was changed (increased: *YJL133C-A*: mitochondrial protein of unknown function; *YJR115W*: paralog of *ECM13*, decreased: *YFR052C-A*: overlaps with the *HXK1* open reading frame) at 25 °C in the absence of Msn2/4 (Fig. 1D).

In the *-Hsf1* strain, the basal transcription of 11 stress response genes was significantly decreased (Fig. 1C,D). The strongest effect was observed for the two indispensable chaperone-encoding genes *SSA2* and *HSC82* whose transcription rate

dropped around 16-fold. All 11 genes whose transcription was found to be dependent on Hsf1 had also been described previously [18] and, as expected, clearly link Hsf1 to the transcriptional regulation of chaperones.

In the absence of all three TFs, the basal transcription of 18 genes (*MSN2* and *MSN4* excluded) was reduced and that of two genes was increased (Fig. 1C, D). One of the decreased genes was the before mentioned *YFR052C-A*. Five genes were only affected when all three TFs were absent which indicates that they are targeted by all three TFs already at 25 °C (Fig. 1C,D). Among them was *CURI* (a paralog of *BTN2*), which is also assumed to be a HDG [18]. With *SSE1* and *HSP12*, two additional stress proteins were found to be redundantly targeted by all three TFs. Furthermore, *UBI4* (ubiquitin) transcription was reduced in the absence of the three transcription factors and this may affect proteasomal turnover. *ADE17* (purine biosynthesis) exhibited increased basal mRNA levels in the absence of all three TFs which potentially indicates a negative regulation of adenosine and ATP levels by the stress-protective TFs.

In summary, our results reveal that all three TFs studied play a specific role in the transcriptional regulation of unstressed cells. Whereas Hsf1 was clearly linked to heat shock proteins as reported previously [18], the deletion of *Msn2* and *Msn4* affected mostly metabolic genes linked to the stress response. In the absence of *Msn2/4*, the barrier to induce sporulation seemed to be decreased. Interestingly, the lack of all three TFs might affect another proteostasis branch, namely degradation, as the *UBI4* transcript levels were basally decreased in this strain. In line with this, we observed an upregulation of *UBI4* under heat stress in the WT strain. Of note, the *UBI1-3* genes, which encode hybrid fusion proteins between unrelated sequences and ubiquitin [54] exhibited a different expression profile (no dependence on Hsf1 and *Msn2/4*).

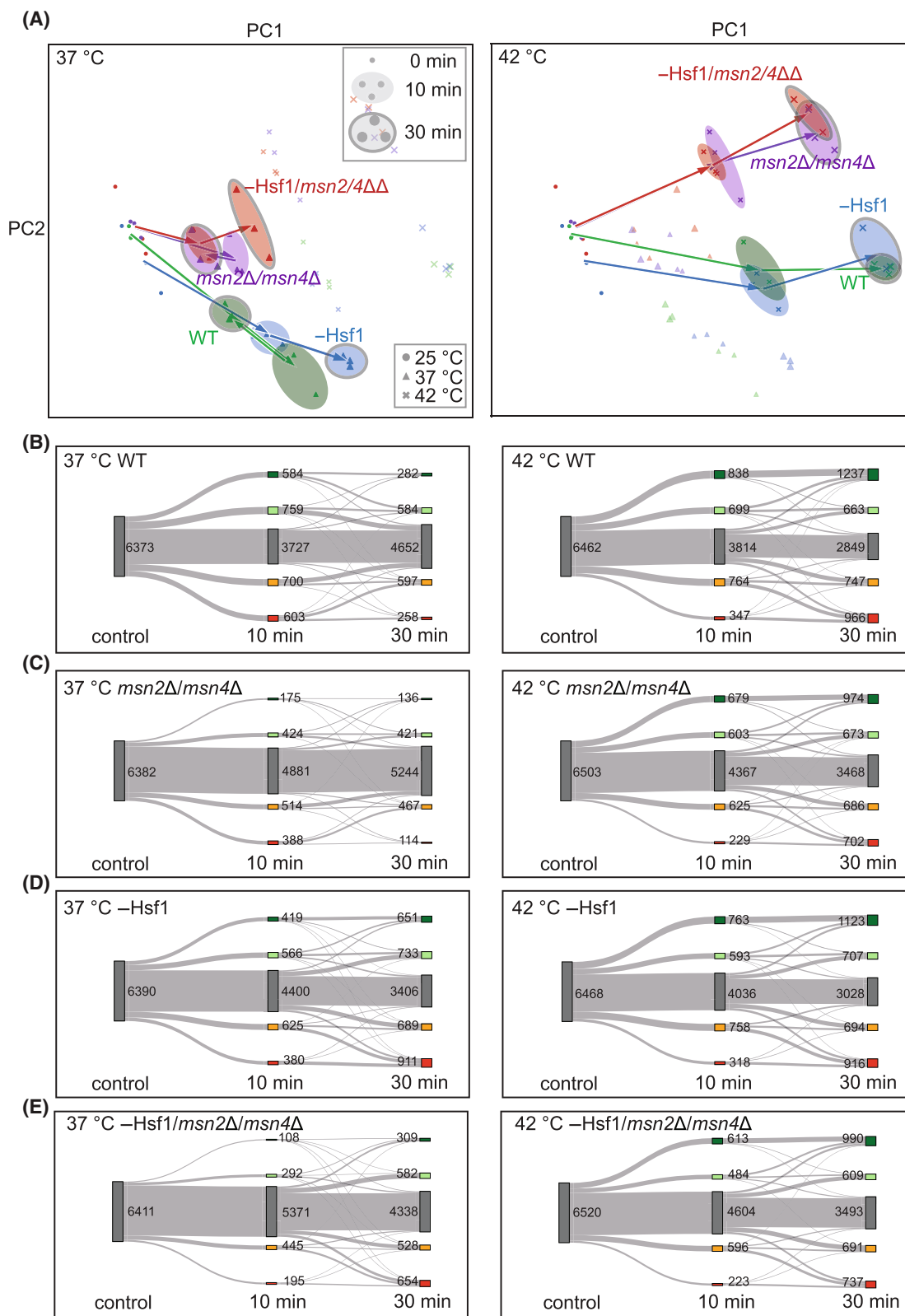
Hsf1 is responsible for the adaptation to mild heat stress

Having determined the genes which depend on the stress transcription factors already under non-stress conditions, we analyzed their influences on the kinetics of the heat shock response (Fig. 2). Cells were subjected to mild (37 °C) or severe (42 °C) heat stress for 0 min (25 °C control), 10 min and 30 min, respectively and changes in expression were determined. To decrease the data complexity due to the many different variables such as genotype, temperature and duration of the stress, we used principal component analysis (PCA) for a general comparison (Fig. 2A). PCA reduces the dimensionality of the data with minimal loss of information and facilitates visualizing the overall trend of the transcriptomes [55]. We observed a separation of the transcriptomes of the different strains based on the genotype, as well as the severity and duration of the stress (Fig. 2A). The sorting of the individual transcriptomes in the PCA analysis was extraordinarily clear; the principal component 1 (PC1) is mainly temperature- and time-dependent. PC2 represents the genotypic difference of the strains with the deletion of *Msn2/4* shaping this component.

In this more detailed view, the data indicate that under mild heat shock conditions (37 °C), more than 2000 genes were up- or downregulated at least two-fold in the WT strain (Fig. 2B and Fig. S2A), similar as described before [10].

Under mild heat shock conditions (37 °C), the response in the WT is initiated within 10 min. The program is successful to adjust to the new conditions as the transcript levels return to physiological levels after 30 min (Fig. 2B). This typical adaptation to mild heat stress [10] was also visible in the PCA (Fig. 2A, overall trends highlighted by the respective arrows) as those transcriptomes approached the unstressed state again

Fig. 2. Cells lacking Hsf1 do not adapt to mild heat stress within 30 min. (A) Mid-logarithmic yeast cells (OD_{595} 0.8) were stressed for 30 min at 37 °C (left) or 42 °C (right). For the depletion of Hsf1, the cells were treated with 1 μ M rapamycin, which was added 45 min before the heat stress was applied. The transcriptome was measured after 0, 10 and 30 min of heat stress in biological triplicates. As a first approximation of the differences in the response to heat shock of each strain, the preprocessed normalized gene counts were visualized via a principal component analysis (PCA). WT (green), *msn2 Δ /msn4 Δ* (purple), $-Hsf1$ (blue), $-Hsf1/msn2 Δ /msn4 $\Delta$$ (red), 25 °C (circles), 37 °C (triangles), 42 °C (crosses). The size of the signs indicates the duration of the stress (small sized: 0 min, medium: 10 min, big: 30 min). The number of changed genes is shown in Fig. S2A. (B–E) In the detailed views, the changes from 10 to 30 min of a strain (WT (B), *msn2 Δ /msn4 Δ* (C), $-Hsf1$ (D), $-Hsf1/msn2 Δ /msn4 $\Delta$$ (E)) during heat shock were analyzed (left: 37 °C, right: 42 °C). Individual genes were classified into several classes, which we describe as ‘no assumption’ ($|\log_2 fc| < 1$), ‘low’ ($1 \leq |\log_2 fc| \leq 2$), or ‘strong’ ($|\log_2 fc| > 2$) regulation of the corresponding gene. The classes are assigned based on up- (green) or downregulated (yellow/red) as determined by DESeq. Genes that did not exhibit significant fold changes were classified as ‘no assumption’ (gray). The classes were plotted as a Sankey diagram to compare the changes in the whole experiment along selected dimensions. An enrichment analysis of the late HSR is shown in Fig. S2C.



(U-turn of the arrow direction). In the Hsf1-depleted strain, the HSR was maintained or even increased during mild heat stress (Fig. 2A,D,E and Fig. S2A). After prolonged stress, the number of genes with changes in transcription was approximately two-fold higher in the Hsf1-depleted cells than in the WT (Fig. S2A). These findings demonstrate that Hsf1 is essential for the adaptation process to mild heat stress.

Deletion of Msn2/4 did not affect the Hsf1-dependent adaptation process (Fig. 2A,C). Thus, all strains in which Hsf1 was present adapted to mild heat stress and the transcriptomes approached the levels observed under physiological conditions again. In the strain lacking all three TFs, the pattern of the response and stress adaptation is comparable to the Hsf1-depleted cells and weakened by a factor of around 3 compared to the WT. Thus, cells lacking all three TFs exhibit only very limited changes in their transcriptomes in response to stress.

Exposing the strains to more severe stress (42 °C) led to changed transcription levels of around 3000 genes in all genotypes (Fig. S2B). As indicated in the PCA, no strain adapted to the severe stress (Fig. 2A). The observed changes were even stronger after prolonged stress (Fig. 2). The kinetics of the responses in the Msn2/4 KO strain and the Hsf1-depleted cells toward severe heat stress were comparable to the WT (Fig. 2B–D). Only the number of changed genes was reduced. Taken together, these results show that in yeast, adaptation to heat stress is only possible under mild heat stress conditions and in the presence of Hsf1.

Hsf1, Msn2, and Msn4 depletion shuts down the core stress response program

Gene by gene comparisons of the stress-induced changes in the transcript levels of the different strains revealed that the stress-responsive program initiated in the cells lacking either Hsf1 or Msn2/4 exhibits a moderate correlation with the WT cells (Fig. 3A,B) corroborating the importance of both Hsf1 and Msn2/4 to the transcriptomic HSR. Moreover, it is also visible in the scatter plots that Msn2/4 targeted more genes than Hsf1 and therefore the correlation between the *msn2Δ/msn4Δ* and the WT transcriptome was worse than between the $-Hsf1$ and the WT strain. Severe heat stress led to a slightly better correlation of the transcriptomic changes in the different genotypes compared to 25 °C indicating that other factors might gain importance at 42 °C (Fig. 3B). The absence of all three TFs led to the weakest correlation: Many genes that were up- and downregulated in the WT remained unchanged in the strain without all three TFs.

As expected, in the WT the upregulated genes were strongly linked to the HSR and comprised many genes involved in *protein folding*, namely HSPs and genes involved in the synthesis of trehalose, as well as glycolytic enzymes. The general picture in the WT was similar at 42 °C (Fig. 2B and Fig. S2B). Thus, the transcriptional reprogramming in WT yeast (a) increases the capacity of folding (b) supports extrinsic protein stabilization *via* trehalose [56], (c) provides additional energy from glycolysis and (d) decreases protein synthesis [9,10]. Additionally, under severe heat stress conditions, genes involved in sporulation were found to be enriched in the WT. To get an overview of pathways targeted by Msn2/4 and Hsf1 under heat shock we determined the gene ontology (GO) sets involved. This analysis revealed that at both temperatures Msn2/4 is responsible for the regulation of the metabolic branch of the HSR [57] including carbohydrate metabolism (Fig. 3C). Under mild heat stress, endocytosis and glycerolipid metabolism are also negatively affected in the absence of Msn2/4 (Fig. 3C).

In addition to the expected lack of the stress-induced upregulation of chaperones in the absence of Hsf1 [18], our analysis showed that Hsf1 induced the upregulation of longevity pathways, the MAP kinase signaling pathway, endocytosis (the latter two only at 37 °C) (Fig. 3C) and protein processing in the ER (42 °C). MAP kinase signaling is in turn involved in a multitude of stress response pathways, resulting e.g. in the enhancement of cell wall integrity and the induction of sporulation [58]. As mentioned above, the Hsf1-depleted strain was not able to adapt to mild heat stress and maintained its stress-responsive program (Figs 2 and 3A). Of note, the Hsf1-dependent chaperone set was also not upregulated after 30 min in the Hsf1-depleted strain. These data suggest that there is a second wave of responses, which targets processes such as protein catabolic processes in the ER or the cell cycle (Fig. S2C). In addition, many of those genes were linked to the cellular response to a chemical stimulus, another stress-responsive branch.

An important aspect of the heat shock response revealed in our analysis is that Msn2/4 and especially Hsf1 play an important role in the repression of genes involved in rRNA processing and ribosome biogenesis indicating that the downregulation of translation at different stages under heat stress is of key importance as it is targeted by all three TFs. Of note, in the Hsf1-depleted strain, Msn2/4 alone still repressed the transcription of these genes and they remained strongly decreased after 30 min at 37 °C (Fig. 3A, blue genes).

The in-depth analysis of the single branches of the HSR confirmed that the transcription of chaperone genes is strongly dependent on Hsf1 and much less on

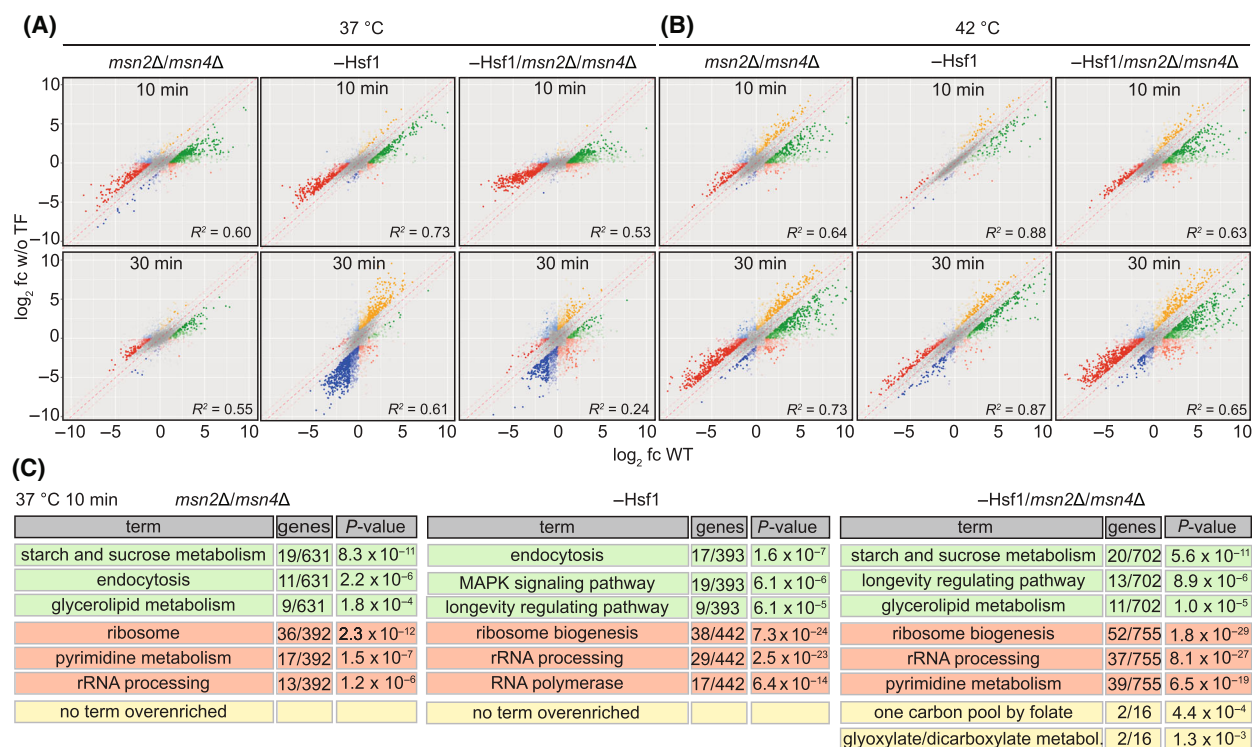


Fig. 3. The comparison of the WT and the mutant transcriptome reveals key processes that are affected by the TFs under heat shock. The scatter plot shows the logarithmic fold changes (\log_2 fc) of one strain (x-axis; WT) against \log_2 fc in another strain (y-axis). The \log_2 fc for the respective strain were determined at a certain time after the heat shock (10/30 min HS) compared to the same strain without HS (0 min). The scatter plot compares a KO strain vs. the WT to show differential regulation of genes in the mutant strain upon HS (A: 37 °C; B: 42 °C). The diagonal line indicates genes that have the same sign and size of \log_2 fc in the two compared strains (double differential change (DDC) = 0). Genes near the diagonal have small differences between strains on HS and are shown in gray (small DDCs). Genes with large differences of the two logarithmic fold changes (large DDCs) in at least one strain (\log_2 fc difference > 1) are shown in color. In principle, we can observe four combinations of regulations in the two strains: upregulated upon HS in both strains (++), upregulated in one and downregulated in the other strains (+-, -+), and downregulated in both strains (--). The two classes with the same direction (++, --) were further divided into two subclasses based on the strain where the regulation is stronger (scatter points above and below the diagonal). These resulting six classes are highlighted with different colors. To keep the quality high in the resulting sets, the fold change in the dominant strain or, in the case of direction change, the fold change in either of the strains had to be significant (adjusted *P*-values < 0.05 and $|\log_2$ fc| > 1). Genes for which both \log_2 fc were significant are represented as filled dots, genes with only one significant \log_2 fc as triangles pointing the direction of regulation on the corresponding axis (for KO strain the triangles are on the y-axis pointing up/down for up-/downregulated genes), and genes without significant \log_2 fc as unfilled dots. The scatter plot visually highlights the number of genes in the respective classes. The Pearson correlations (R^2) are indicated in the plots. (C) Pathway analysis was performed for each of the six classes independently with hypergeometric tests to test for gene set enrichment of the colored genes in sets derived from both GO [94] and KEGG [95]. The top three terms are displayed.

Msn2/4 (Fig. 4A and Fig. S3A). However, this did not hold true for the small heat shock proteins Hsp26 and Hsp42. Their genes were targeted by Hsf1 as well as by Msn2/4 (Fig. 4B and Fig. S3A) pointing to their importance in different aspects of the stress response like the sequestration of proteins [59,60]. Moreover, they function in the absence of a pronounced stress and can be regulated by posttranslational modification [10,61–65]. Furthermore, the response to oxidative stress and the upregulation of trehalose biosynthesis and glycolysis were mainly regulated by Msn2 and Msn4 as expected. Interestingly, Msn2/4 suppressed

genes involved in proteasome-mediated proteolysis while Hsf1 induced the transcription of several of those genes (Fig. 4A). Analysis of the proteasomal genes that were still upregulated in the absence of the three TFs pointed toward Rpn4 as the responsible TF, which is known to be an important transcriptional regulator for proteasomal genes [66].

Apart from the differences due to the adaptation process to mild heat stress as well as the transcription of genes belonging to meiosis (Fig. 4A) and those associated with sporulation which were differently regulated in the mutant strains (Fig. S3A), our study

revealed that more than 50% of the upregulated Hsf1 targets overlapped with Msn2/4 targets after 10 min at 37 °C (Fig. S3B). Therefore, we could identify many genes that were regulated redundantly by Msn2/4 and Hsf1 (Fig. S3B). This stresses the importance of this central and overarching stress-protective transcriptional program. Of note, the number of Msn2/4 target genes was about twice as high as that of Hsf1. Even though, in the strain lacking all three stress TFs, the transcription of numerous genes was still found to be increased under HS conditions (Figs 2 and 3), while the core stress response comprising chaperones and trehalose biosynthesis was absent in this strain.

The repression of genes under stress is even more redundant. Around 2/3 of the Hsf1-repressed and roughly 1/2 of the Msn2/4-repressed genes are also repressed by the other TF (37 °C, 10 min; Fig. S3B). Those 221 genes were only unchanged in the absence of all three TFs which supports a more general gene repression function shared by Hsf1 and Msn2/4 mainly targeting processes linked to translation. Importantly, there are still 437 genes whose levels are still reduced even though Hsf1 and Msn2/4 were absent which indicates that there are further important TFs involved.

In summary, the deletion of Msn2/4 negatively affected the metabolic branch of the HSR whereas Hsf1 was essential for the efficient upregulation of the chaperone branch (Fig. 4C) as it was expected. In consequence, this core HSR which mainly comprises chaperones, trehalose biosynthesis enzymes as well as glucose metabolism enzymes was switched off only when all three TFs were absent. Together they are also required to suppress translation, ribosome biogenesis and RNA processing. Notably, in the absence of all three TFs, several genes involved in sporulation were still found to be increased under stress indicating the existence of an additional emergency-escape program, which is not regulated by Hsf1 and Msn2/4.

Several hundred proteins aggregate in the absence of Hsf1 and Msn2/4

It is generally assumed that the major task of the HSR is to avoid deleterious consequences of stress on the proteome. Our deletion strains put us in the position to investigate the effects of heat stress on a largely unprotected proteome and to directly determine the proteins that aggregated in the absence of a major part of the stress response. For the proteome analysis, the cells (WT and the strain lacking Hsf1 and Msn2/4) were again subjected to mild (37 °C) or severe (42 °C) heat stress for 0 (25 °C control), 30 or 60 min, respectively. Label-free quantification mass spectroscopy

(LFQ-MS) analyses revealed that in the WT yeast strain, the levels of more than 200 proteins were increased under mild heat shock (37 °C) compared to the unstressed cells, among them many chaperones (Fig. S4A). In contrast, in the strain lacking the three stress-protective TFs, only a few proteins (13) exhibited increased levels (\log_2 fc > 1; P -value < 0.05) and chaperones were not upregulated (Fig. 5A). Thus, stress-induced protein upregulation was strictly dependent on the action of Msn2/4 and Hsf1. The two most significant hits among the upregulated proteins were Hac1 and Rts3. Rts3 is a putative component of the protein phosphatase 2A [67] and was already conspicuous in the transcriptome analysis. Interestingly, PP2A is known to activate Msn2 [53]. Hac1 is the key TF activated by the unfolded protein response (UPR) [68].

Hac1 was also slightly increased upon heat shock at the transcriptomic level and Ire1, which splices Hac1, was upregulated in the absence of the HSR transcription factors. Interestingly, the successful splicing of *HAC1* was clearly visible in the transcriptome as intron reads were not present anymore in the strain without Msn2/4 and Hsf1 at 37 and 42 °C, as well. Hence, the observed proteomic change of Hac1 is in line with the transcriptome data.

At 42 °C, fewer proteins were increased in the WT (33), and only 10 proteins in the strain lacking Hsf1 as well as Msn2/4 (Fig. 5A). Hac1 and Rts3 were again the most significant hits. Notably, sporulation was not found to be upregulated at the level of the proteome.

MS analysis of the insoluble fraction after heat stress showed that many different proteins aggregated in the strain lacking all three TFs (Fig. 5B). While in the WT strain after 30 min at 37 °C, 137 proteins were found in the insoluble fraction, around 240 proteins were found pellet-enriched in the strain lacking all three TFs (Fig. 5B,C and Fig. S4B). At 42 °C, the amount of proteins found in the insoluble fraction of the WT strain (193) was comparable to the mutant strain (222) after 30 min (Fig. 5B,C and Fig. S4B). While in the case of the WT strain, the stress protection was already limited at this temperature, in the mutant strain the proteome was hardly stress-protected at any point which becomes obvious especially under mild heat stress. This led to a rather small overlap of aggregating proteins in the two strains. After 60 min of heat stress even more proteins were found in the pellet fraction of the strain without the three TFs (Fig. 5C): 401 proteins at 37 °C and 323 proteins at 42 °C, were 146 and 165 proteins respectively in the WT strain (Fig. 5C). Thus, the solubility of several hundred proteins is ensured by the heat shock response. A pointwise comparison (scatter plot) of the

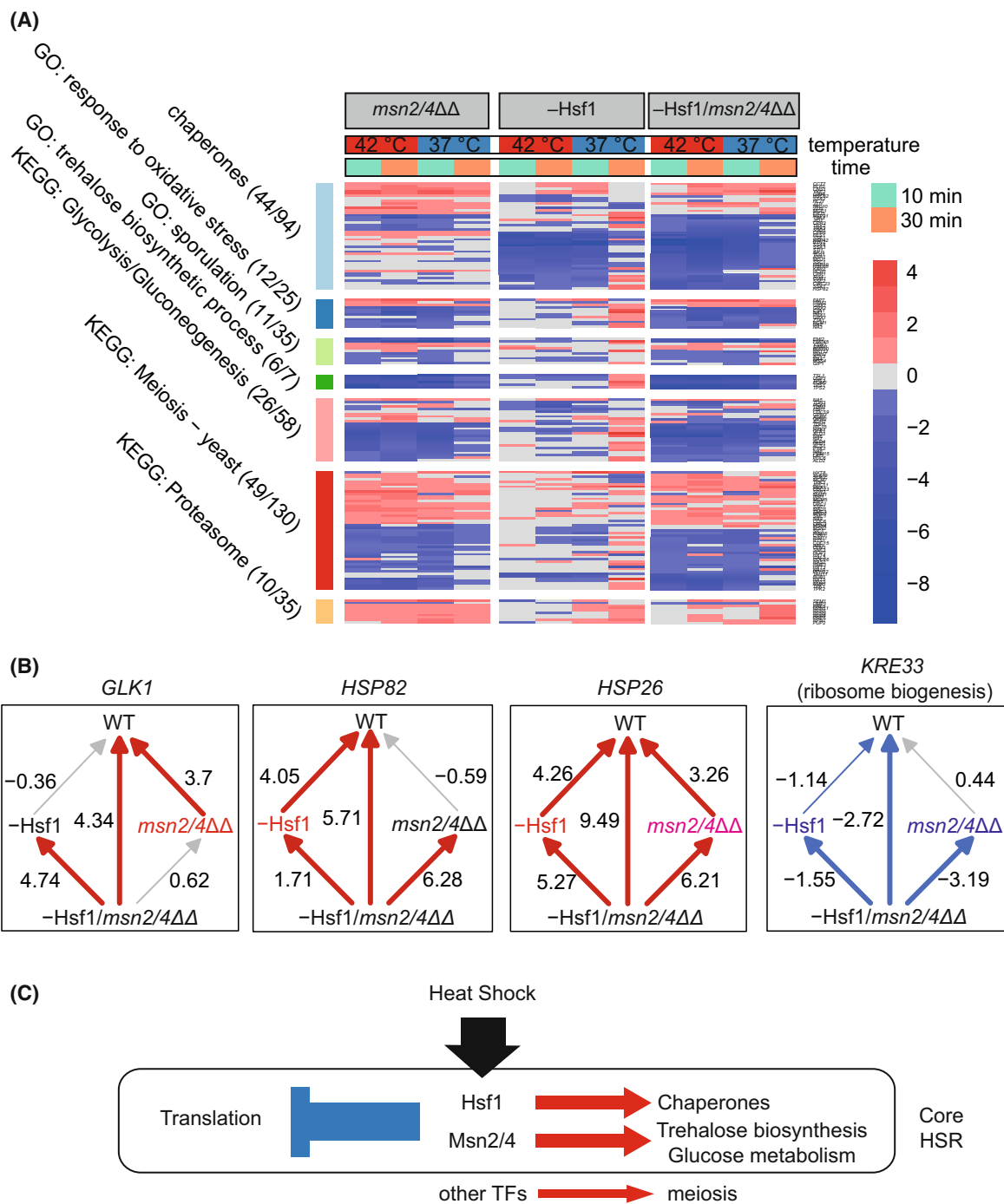


Fig. 4. The core heat shock response is switched off in cells lacking Hsf1 and Msn2/4. (A) Core regulatory information was extracted and the difference in fold changes between mutant strains and the WT were visualized with a heat-map. To highlight the genes with the largest changes between strains, only genes with a 90% confidence interval of all \log_2 fold-change differences between strains greater than 1 were selected. A more detailed expression component analysis (ECA) of selected biological categories can be found in Fig. S3A. (B) The function of ECA is depicted for representative genes of the main TF target classes. All required fold changes were calculated by DESeq and arrows are red if the \log_2 fold change is greater than 1 and blue if it is less than -1. Arrows were drawn thick if they had an adjusted *P*-value below 0.05. (C) Schematic view of the regulation of the HSR by Msn2/4 and Hsf1. Hsf1 is responsible for the chaperone branch and Msn2/4 for the metabolic branch. Together, those two branches are referred to as the 'core HSR'. A main function of the remaining rest regulation seems to be the escape into sporulation. The overlap of the gene targets of the different TFs is shown in Fig. S3B.

insoluble proteomes after 30 and 60 min confirmed that the aggregation phenotype was aggravated under prolonged stress (Fig. S4C).

A comparison of the aggregating proteins in the WT and the strain lacking the three TFs revealed that most of the proteins that were pellet-enriched uniquely in the WT belong to the stress-protective machinery (Fig. 5C) consistent with their interaction with non-native proteins during stress. As those proteins were not upregulated in the strain lacking the responsible TFs they were also not enriched in the pellet fraction of the mutant strain. The pellet-enriched proteins in this strain were connected to cell cycle and growth, which might be another explanation for the observed stop of cell growth under stress (Fig. 1C).

We next analyzed the aggregating proteins in more detail to identify common features that make proteins chaperone-dependent. We found that up to 22% of the aggregating fraction of the strain without the three TFs were cofactor-binding proteins [69] (Fig. 6A). Of all identified proteins in this experiment only 12% were cofactor-binding. Of note, cofactor insertion in proteins is a process known to involve chaperones [70–72]. It should be noted that also in the pellet fraction of WT cells the percentage of proteins with cofactors was increased (37 °C 30 min: 15.4%; 37 °C 60 min: 13.1%; 42 °C 30 min: 16.0%; 42 °C 60 min: 17.6%) but not as pronounced as in the strain without the three TFs. For most of the pellet-enriched proteins, either Zn²⁺, Mg²⁺, PLP or FAD were annotated as the cofactor (Fig. 6A).

Another intriguing finding was that the presence of intrinsically disordered regions (IDR) in a protein seems to affect the chaperone dependency under stress (Fig. 6B). Among all detected proteins, around 52% contained IDRs longer than 19 aa [73]. While the ratio of IDRs detected in the pellet of the WT cells stressed for 60 min at 37 °C was similar to the average value,

this value dropped to around 40% in the pellet of the mutant strain (Fig. 6B). This implies that especially proteins with ordered structures are enriched in the pellet when chaperones are absent. Thus, structured proteins depend more on chaperoning under stress than IDR-containing proteins. Similar effects were observed at 42 °C, whereas at this more severe stress temperature, the difference between WT and the mutant strain was smaller (Fig. 6B).

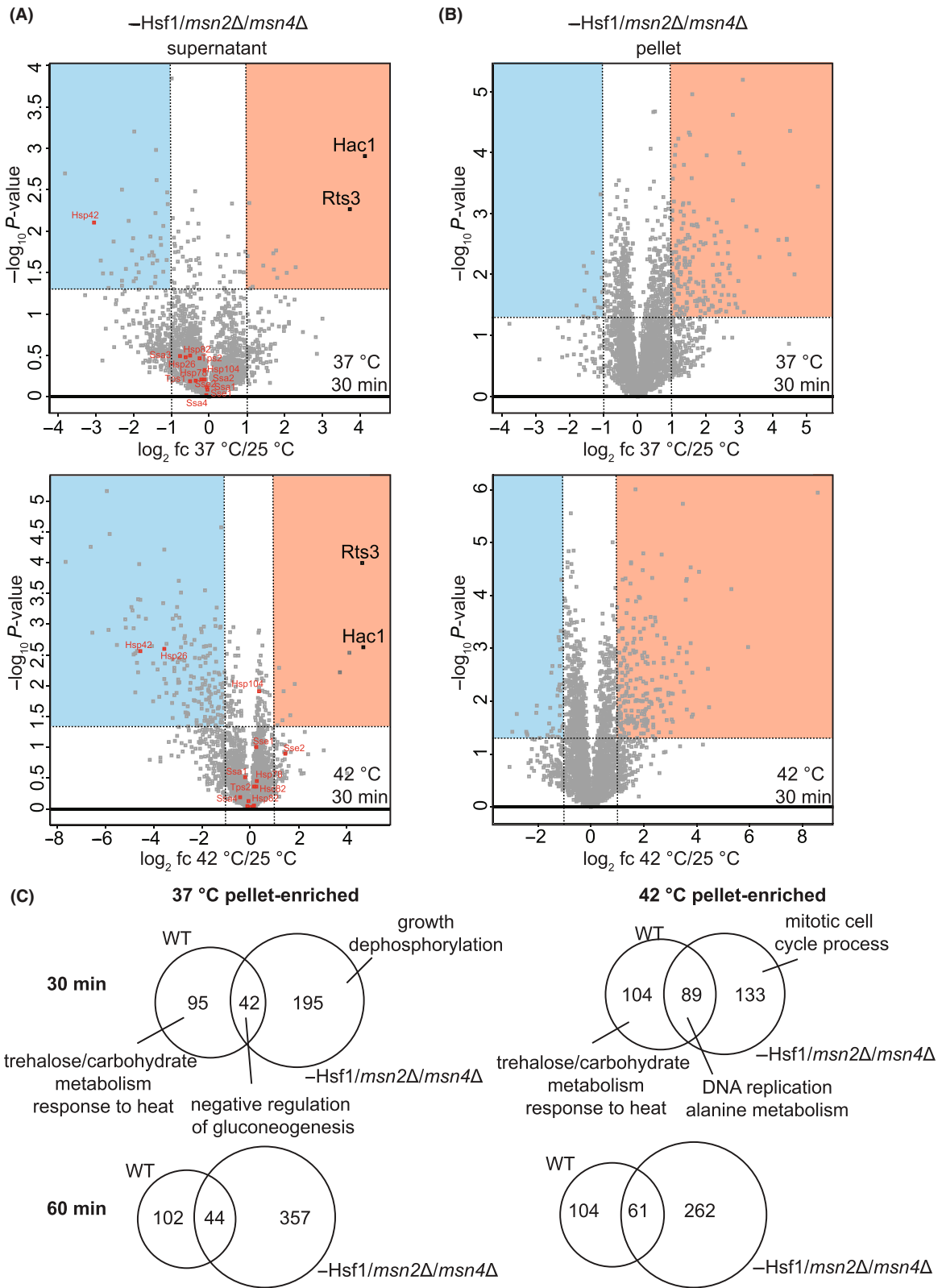
The most striking difference in the composition of the pellet fraction was the enrichment of essential proteins in the strain lacking the three TFs at 37 °C. In WT cells after 30 min of mild heat stress, only 5.9% of the aggregating proteins were essential according to the DEG database [74]. In contrast, the percentage of essential genes was more than three times higher in the strain without the three TFs (20%) (Fig. 6C). The essential proteins aggregating in the strain lacking the stress response were mainly linked to genome replication, segregation and mRNA processing. This protective effect seemed to be specific for mild heat stress, as at 42 °C the amount of aggregated essential proteins was similar in both strains. Again, the aggregated essential proteins were mainly involved in DNA replication and double strand break repair, in the mutant as well as in the WT.

In summary, the number of aggregating proteins was strongly increased when yeast cells were not able to initiate a proper stress response anymore. The proteomic analyses revealed that certain proteins are specifically prevented from forming insoluble aggregates by the heat shock response.

Discussion

Recently, a seminal paper revealed that the number of Hsf1-dependent genes in yeast is much smaller than

Fig. 5. The absence of Hsf1 and Msn2/4 results in massive aggregation processes at 37 °C. (A) Hsf1 was depleted by the addition of 1 μ M rapamycin in the *msn2 Δ /msn4 Δ* strain and the yeast cells were stressed for 30 min at 37 °C (upper panel) or 42 °C (lower panel). The soluble fraction was analyzed with LFQ-MS/MS. Fold changes were calculated with the proteome of cells kept at 25 °C as a base. The experiments were performed in biological triplicates and a two-sided *t*-test was performed. The red box indicates significantly upregulated proteins (\log_2 fc > 1; *P*-value < 0.05) and the blue box comprises downregulated proteins (\log_2 fc < -1; *P*-value < 0.05). Selected chaperones are shown in red. The two most significant upregulated proteins Rts3 and Hac1 are indicated in black. In Fig. S4A the corresponding experiment with WT cells is shown. (B) LFQ-MS/MS analysis of the insoluble protein fraction. Fold changes were calculated with the insoluble proteome of cells kept at 25 °C as a base. The experiments were performed in biological triplicates and a two-sided *t*-test was performed. The red box indicates pellet-enriched proteins (\log_2 fc > 1; *P*-value < 0.05) under stress and the blue box comprises proteins that appeared to be depleted from the pellet (\log_2 fc < -1; *P*-value < 0.05). In Fig. S4B the corresponding experiment with WT cells is shown. (C) Comparison of the insoluble protein fractions of WT and *-Hsf1/msn2 Δ /msn4 Δ* cells stressed at 37 or 42 °C for 30 or 60 min, respectively. The number of proteins in each fraction as well as the main GO terms are indicated in the Venn diagrams [96]. Comparisons of the insoluble protein fractions of *-Hsf1/msn2 Δ /msn4 Δ* cells stressed for 30 and 60 min are shown as scatter plots in Fig. S4C.



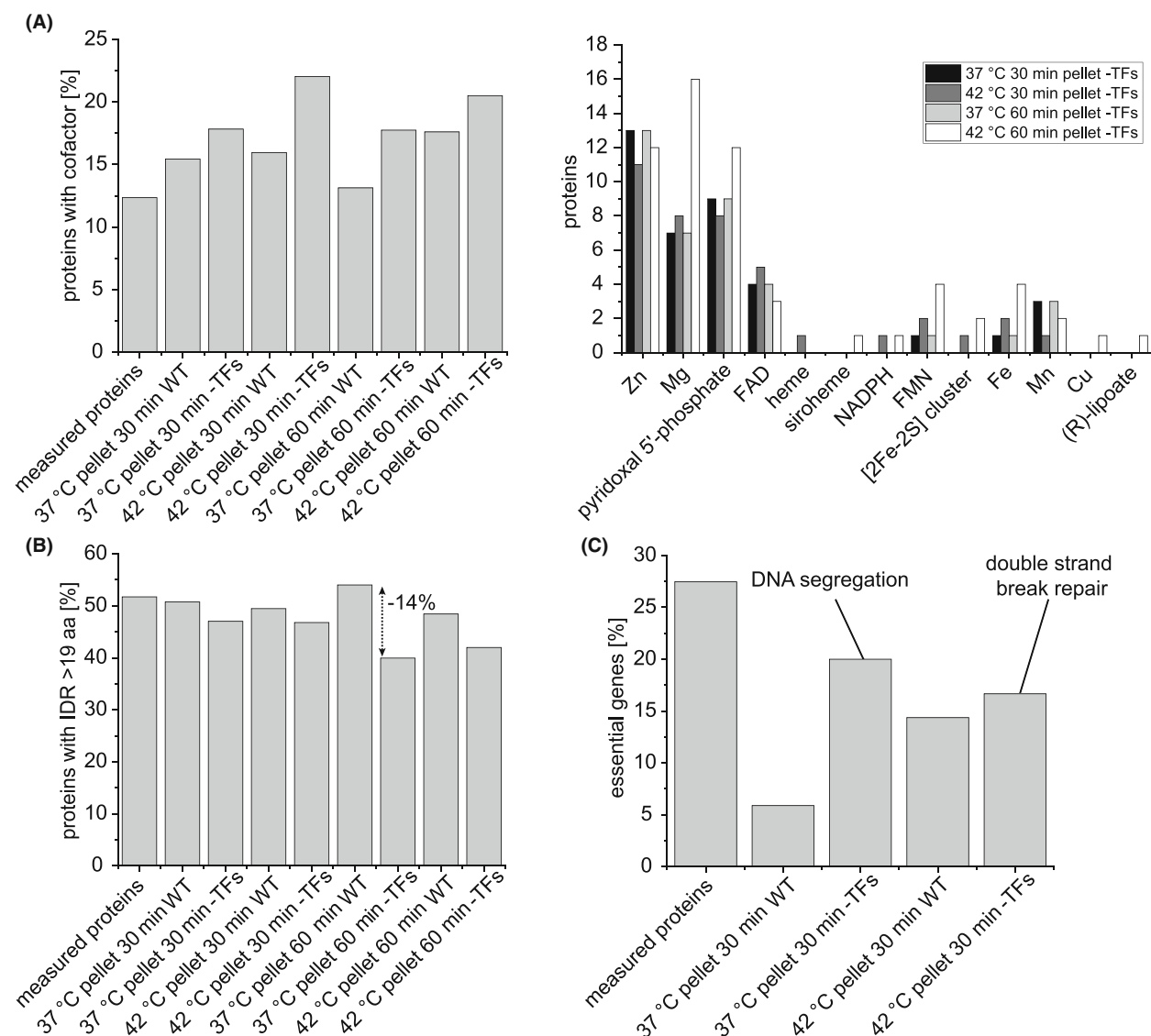


Fig. 6. Essential proteins depend on chaperones under stress. (A) Pellet-enriched proteins ($\log_2 fc > 1$, P -value < 0.05) were analyzed based on the content of cofactor binding proteins (according to Uniprot DB). In the right panel, the main cofactors are shown. (B) Pellet-enriched proteins ($\log_2 fc > 1$, P -value < 0.05) were analyzed based on the content of intrinsically disordered regions (IDR) [73]. (C) Pellet-enriched proteins ($\log_2 fc > 1$, P -value < 0.05) were analyzed based on the content of essential genes according to the DEG database [74]. The main GO terms of the essential proteins that are aggregating in the mutant strain are indicated in the plot [96]. -TFs is short for $-Hsf1/msn2\Delta/msn4\Delta$.

expected [18]. This begs the questions what the contribution of the two stress-related TFs Msn2 and Msn4 is, to what extent they fulfill an overlapping function and how yeast would tolerate stress in the absence of all of them. We therefore studied the target spectra and the interplay of those three TFs in detail. Our global analyses revealed that in the absence of all three TFs, yeast cells are unable to initiate the core stress-responsive program, which includes molecular chaperones, trehalose biosynthesis as well as glycolytic

enzymes (Fig. 7). Thus, the three TFs together indeed orchestrate the overall general stress response. Consistent with the literature, the Hsf1-induced program is specific for HSPs and Msn2/4 initiate a more general transcriptional program [18,24–26]. We could show that the target spectrum of the TFs does not seem to be dependent on the severity of the stress. However, we observed that the amplitude of the gene regulatory response and the possibility for the cell to adapt correlate with the stress intensity in line with previous

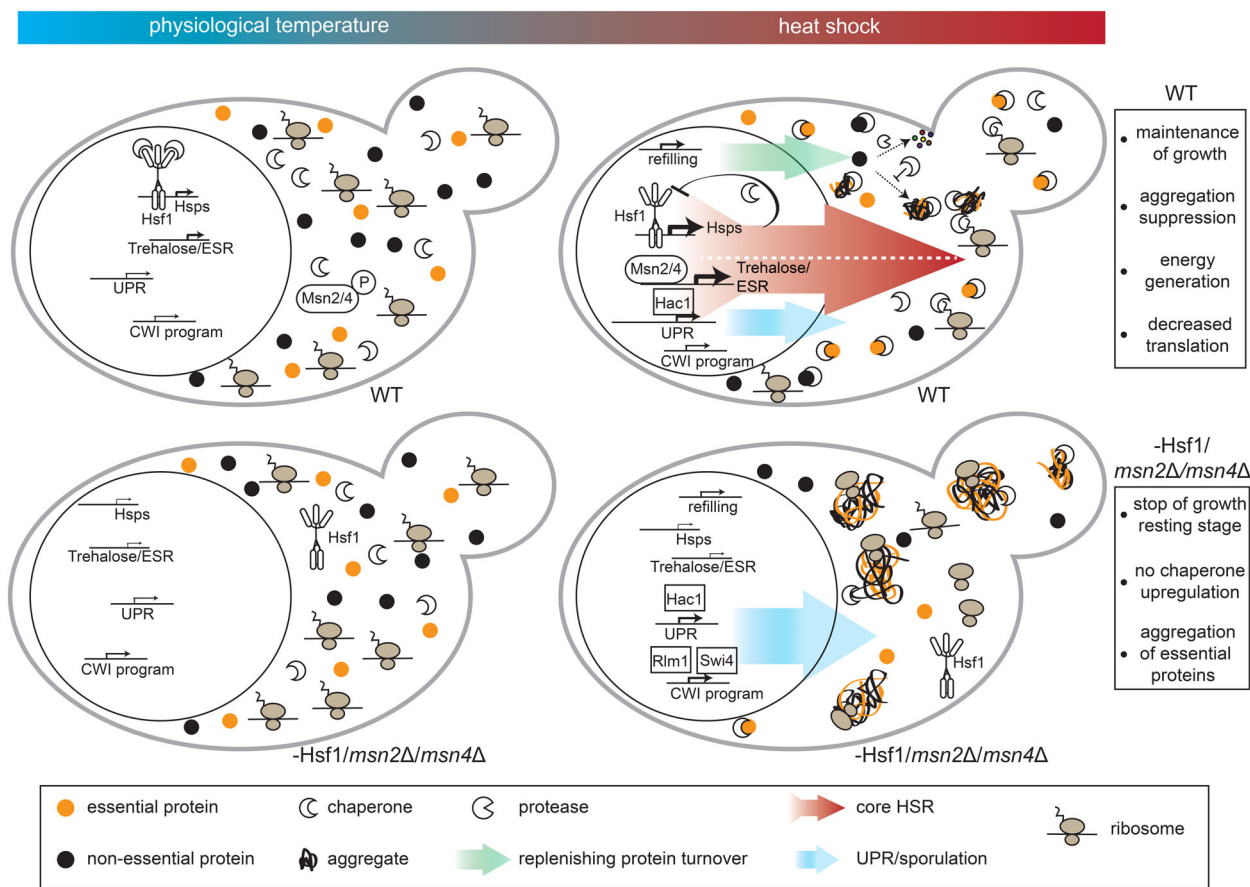


Fig. 7. Schematic model of the effects of heat stress on yeast cells in the presence and the absence of a stress-protective program. On the left unstressed cells are shown (upper cell: WT, lower cell: strain without Hsf1 and Msn2/4). Already at permissive temperature, the levels of several stress-protective proteins were decreased. On the right stressed cells are shown. WT cells induce a stress-protective program, which is mainly orchestrated by Hsf1 and Msn2/4. Upregulation of chaperones and trehalose biosynthesis strongly supports the maintenance of proteostasis. The cells lacking the stress-responsive transcription factors were much more stress-sensitive, which resulted in severe protein aggregation, especially of essential proteins and under mild heat stress. Those cells enter a dormant stage and the rest stress-responsive program is initiated by the cell wall integrity pathway (CWI) as well as the integrated stress response (ISR) and the unfolded protein response (UPR).

findings for WT yeast cells [10]. In this work, we identified Hsf1 to be responsible for the adaptation to mild heat stress as in its absence the cells maintain their stress-responsive program for prolonged periods of time. Thus, even though only a few genes are regulated uniquely by Hsf1, this group of genes, especially chaperones, plays a very important role for adaptation, in line with the chaperone titration model for the regulation of Hsf1 [75]. Specifically, chaperone recruitment toward misfolded newly synthesized proteins has been identified to be the main trigger for the activation of Hsf1 [76]. Based on the extent of the adaptation process one could imagine that the negative feedback loop by Hsf1-induced chaperones might be expanded to other stress-responsive transcription factors. e.g. for Msn2 and/or Msn4 physical interaction with Hsc82,

Hsp82, and Ssa1 was reported [77,78] which supports this idea. The deletion of Msn2/4 led to more changes in the transcriptome as it was expected from previous reports [9,27]. We could confirm that those genes seemed to be less important for acute survival as no severe growth phenotype was observed under stress [28] and that Hsf1 as well as Msn2/4 also regulate gene transcription under physiological conditions [18,79].

The picture emerging is that together they exhibit protective core functions under all conditions, whereas Hsf1 seems to play a more strategic role. Thus, there is no clear separation between a physiological situation that does not require the support of the stress response at all and non-physiological, proteotoxic conditions. Rather, the protective system is more or less engaged

depending on the demands on energy and protection and only the amplitude of engagement is adjusted.

It was still debated to what extent the target spectra of Hsf1 and Msn2/4 are overlapping [29,80,81]. Our analysis confirmed that there are specific sets of Hsf1 targets (chaperones) and Msn2/4 targets (e. g. carbohydrate metabolism). In addition, we could show that around 25–33% of the Msn2/4 targets and at least half of the Hsf1 targets are also targeted by the other TF. As a consequence, for those genes, which were e.g. linked to metabolism or the (oxidative) stress response, the absence of either Hsf1 or Msn2/4 could be balanced by the other TF. The overlapping function of the three stress-responsive factors was even more pronounced concerning the suppression of genes involved in translation indicating that limiting protein synthesis under stress is of key importance. The stress-responsive TFs are furthermore involved in the transcriptional repression of growth-related genes to stop cell growth and division. Together, this represents a defined shut-down that alleviates pressure on the proteome and the energy status of the cell.

Analysis of the stress-induced transcripts of cells lacking the three TFs pinpointed sporulation as a remaining upregulated process. Especially genes targeted by the TFs Rlm1 and Swi4 tended to be upregulated. Whereas Rlm1 is linked to the regulation of cell wall stress-responsive genes, Swi4 is connected to cell cycle and sporulation [82]. Thus, we suggest that the remaining stress signaling is activated by the cell wall integrity pathway (CWI) consistent with the notion that heat is an inducer of the CWI [83]. Moreover, our TF analysis of the remaining transcripts with increased levels under stress suggests a crosstalk with the oxidative stress response *via* Yap1. Among the TFs that were involved after prolonged stress, we also found Gcn4, which responds to environmental changes and induces the transcription of amino acid biosynthesis genes [84]. Of note, Gcn4 becomes active when eIF2 α is phosphorylated whereas phosphorylation of eIF2 α generally inhibits translation initiation under stress [84,85]. Obviously, all those pathways could not compensate the lack of Msn2/4 and especially Hsf1. In this work, we were especially interested in the HSR transcription factors and therefore focused on the transcriptomic changes that are associated with a shift in the transcription of target genes. Beyond that, it should be mentioned that stress-induced alterations in mRNA turnover and stability also directly affect the cellular transcriptome.

Recently, we hypothesized that the discrepancy that is observed between the transcriptomic and the proteomic changes under heat stress is due to increased

protein turnover and aggregation under stress, which is replenished by protein synthesis [10]. Around 20% of the proteins that we previously grouped in the category ‘less stable proteins’ whose turnover was balanced by translation, were now reduced in the supernatant of the mutant strain [10]. This indicates that the proteostasis system becomes more fragile due to the absence of stress-protective chaperones and that the suggested ‘refilling reactions’ are impaired to some extent in the absence of the three HS TFs. Of note, heat shock does not only lead to changes in the abundance of cellular proteins but also in the structural dynamics of the proteome [86]. It is reasonable to assume that in addition to strongly affecting the amount of changed proteins, the absence of Hsf1 and Msn2/4 also has a big impact on the conformational ensemble as stabilizing chaperones are not present anymore. Indeed, our analysis revealed that proteins with intrinsically disordered regions may be less dependent on chaperones under stress. Thus, under stress, IDRs which are more charged and less hydrophobic than folded segments can be favorable for colloidal stability in comparison to folded proteins similar as reported in other recent studies [87,88]. However, this may differ under physiological conditions where Hsp90 has been shown to bind IDR-containing proteins [78]. According to our results, this solubility advantage stands out in the mutant strain that is not able to initiate the core HSR. In contrast, we found that proteins binding cofactors were more aggregation-prone in the absence of the three TFs, pointing toward the chaperone-dependence of cofactor binding and folding [70–72]. Another intriguing finding was that essential proteins were especially enriched in the pellet in the absence of chaperones, which indicates that chaperones are important to protect these proteins. Therefore, the data suggest a fine-tuning of the chaperone machinery on essential proteins in yeast. Our findings are supported by previous reports that many proteins are expressed at their solubility limits or even slightly above [89]. Increasing the temperature represents a big challenge for such supersaturated protein solutions and can lead to their breakdown [90]. Using our HSR-deficient strain we could show how molecular chaperones shift the balance of the supersaturated system. In addition, we were able to directly quantify the big impact of the absence of chaperones on the insoluble proteome especially under mild heat stress. At the proteomic level, only a few proteins were still found to be upregulated in the absence of the stress-responsive TFs. Among them, Rts3 and Hac1 were the most significant hits. Rts3 is upregulated to activate the Msn transcription factors *via* PP2A which is of course not successful in a

strain lacking Msn2 and Msn4. Upregulation of Hac1 clearly indicates that the unfolded protein response *via* Ire1 is initiated due to heat-induced protein unfolding in the ER [68]. Heat shock-induced splicing of the *HAC1* transcripts by Ire1 was also visible in the transcriptome datasets as under stress the *HAC1* introns were not present anymore. The transcriptomic upregulation of sporulation genes was not reflected in the proteome, possibly due to a stress-induced stop of translation [85].

Our data reveal that in the absence of the core heat stress response, the cells initiate an emergency program intending to rescue them into sporulation including the induction of the cell wall integrity pathway (Swi4, Rlm1), the unfolded protein response (Hac1) and the oxidative stress response (Yap1) [68,82,91]. Even though we could show that proteostasis is strongly challenged, especially under mild heat stress, this rescue program still allows yeast cells to survive transient heat stress conditions in a resting stage.

Acknowledgements

This work was performed within the frameworks of SFB 1035 (German Research Foundation DFG, SFB 1035, Project number 201302640, project A06), Bioinformatics analysis was partially supported by SFB 1123/2 (DFG, project Z02). We are grateful to Dr David Pincus (University of Chicago) for generously providing the Hsf1 anchor away strain. We thank Bettina Richter and Laura Meier for technical assistance and Katja Bäuml for operating the mass spectrometer. We thank Dr Stefan Krebs (Gene Center, LMU Munich) for NGS. Moritz Mühlhofer was supported by a fellowship of the Studienstiftung des deutschen Volkes. Open Access funding enabled and organized by Projekt DEAL.

Author contributions

MM, GC, EB, MH, RZ and JB designed the study. HB designed the transcriptome study. MM, MR and SR performed the experiments. GC, FO, EB and GW processed the NGS data. MM, SR, GC, FO, EB, HB, MH, RZ and JB evaluated the data. MM, FO, MH, RZ and JB wrote the manuscript.

Data accessibility

The mass spectrometry proteomics data have been deposited to the ProteomeXchange Consortium *via* the PRIDE partner repository [92] with the dataset identifier PXD024352. Transcriptomic sequencing data

discussed in this publication have been deposited in NCBI's Gene Expression Omnibus [93] and are accessible through GEO Series accession number GSE179258. Link: <https://www.ncbi.nlm.nih.gov/geo/query/acc.cgi?acc=GSE179258>.

References

- Morano KA, Grant CM and Moye-Rowley WS (2012) The response to heat shock and oxidative stress in *Saccharomyces cerevisiae*. *Genetics* **190**, 1157–1195.
- Richter K, Haslbeck M and Buchner J (2010) The heat shock response: life on the verge of death. *Mol Cell* **40**, 253–266.
- Field SB and Anderson RL (1982) Thermotolerance: a review of observations and possible mechanisms. *Natl Cancer Inst Monogr* **61**, 193–201.
- Plesset J, Palm C and McLaughlin CS (1982) Induction of heat shock proteins and thermotolerance by ethanol in *Saccharomyces cerevisiae*. *Biochem Biophys Res Commun* **108**, 1340–1345.
- Lindquist S (1986) The heat-shock response. *Annu Rev Biochem* **55**, 1151–1191.
- Tissières A, Mitchell HK and Tracy UM (1974) Protein synthesis in salivary glands of *Drosophila melanogaster*: relation to chromosome puffs. *J Mol Biol* **84**, 389–398.
- Hartl FU, Bracher A and Hayer-Hartl M (2011) Molecular chaperones in protein folding and proteostasis. *Nature* **475**, 324–332.
- Labbadia J and Morimoto RI (2015) The biology of proteostasis in aging and disease. *Annu Rev Biochem* **84**, 435–464.
- Gasch AP, Spellman PT, Kao CM, Carmel-Harel O, Eisen MB, Storz G, Botstein D and Brown PO (2000) Genomic expression programs in the response of yeast cells to environmental changes. *Mol Biol Cell* **11**, 4241–4257.
- Mühlhofer M, Berchtold E, Stratil CG, Csaba G, Kunold E, Bach NC, Sieber SA, Haslbeck M, Zimmer R and Buchner J (2019) The heat shock response in yeast maintains protein homeostasis by chaperoning and replenishing proteins. *Cell Rep* **29**, 4593–4607.e8.
- Morimoto RI (1998) Regulation of the heat shock transcriptional response: cross talk between a family of heat shock factors, molecular chaperones, and negative regulators. *Genes Dev* **12**, 3788–3796.
- Gomez-Pastor R, Burchfiel ET and Thiele DJ (2018) Regulation of heat shock transcription factors and their roles in physiology and disease. *Nat Rev Mol Cell Biol* **19**, 4–19.
- Vihervaara A and Sistonen L (2014) HSF1 at a glance. *J Cell Sci* **127**, 261–266.
- Verghese J, Abrams J, Wang Y and Morano KA (2012) Biology of the heat shock response and protein

- chaperones: budding yeast (*Saccharomyces cerevisiae*) as a Model system. *Microbiol Mol Biol Rev* **76**, 115–158.
- 15 Jakobsen BK and Pelham HRB (1988) Constitutive binding of yeast heat shock factor to DNA in vivo. *Mol Cell Biol* **8**, 5040–5042.
 - 16 Akerfelt M, Morimoto RI and Sistonen L (2010) Heat shock factors: integrators of cell stress, development and lifespan. *Nat Rev Mol Cell Biol* **11**, 545–555.
 - 17 Sorger PK and Pelham HRB (1988) Yeast heat shock factor is an essential DNA-binding protein that exhibits temperature-dependent phosphorylation. *Cell* **54**, 855–864.
 - 18 Solís EJ, Pandey JP, Zheng X, Jin DX, Gupta PB, Airoidi EM, Pincus D and Denic V (2016) Defining the essential function of yeast Hsf1 reveals a compact transcriptional program for maintaining eukaryotic Proteostasis. *Mol Cell* **63**, 60–71.
 - 19 Kobayashi N and McEntee K (1993) Identification of cis and trans components of a novel heat shock stress regulatory pathway in *Saccharomyces cerevisiae*. *Mol Cell Biol* **13**, 248–256.
 - 20 Wieser R, Adam G, Wagner A, Schüller C, Marchler G, Ruis H, Krawiec Z and Bilinski T (1991) Heat shock factor-independent heat control of transcription of the CTT1 gene encoding the cytosolic catalase T of *Saccharomyces cerevisiae*. *J Biol Chem* **266**, 12406–12411.
 - 21 Schmitt AP and McEntee K (1996) Msn2p, a zinc finger DNA-binding protein, is the transcriptional activator of the multistress response in *Saccharomyces cerevisiae*. *Proc Natl Acad Sci U S A* **93**, 5777–5782.
 - 22 Estruch F and Carlson M (1993) Two homologous zinc finger genes identified by multicopy suppression in a SNF1 protein kinase mutant of *Saccharomyces cerevisiae*. *Mol Cell Biol* **13**, 3872–3881.
 - 23 Martínez-Pastor MT, Marchler G, Schüller C, Marchler-Bauer A, Ruis H and Estruch F (1996) The *Saccharomyces cerevisiae* zinc finger proteins Msn2p and Msn4p are required for transcriptional induction through the stress response element (STRE). *EMBO J* **15**, 2227–2235.
 - 24 Boy-Marcotte E, Perrot M, Bussereau F, Boucherie H and Jacquet M (1998) Msn2p and Msn4p control a large number of genes induced at the diauxic transition which are repressed by cyclic AMP in *Saccharomyces cerevisiae*. *J Bacteriol* **180**, 1044–1052.
 - 25 Kandró O, Bretschneider N, Kreydin E, Cavaliere D and Goldberg AL (2004) Yeast adapt to near-freezing temperatures by STRE/Msn2, 4-dependent induction of trehalose synthesis and certain molecular chaperones. *Mol Cell* **13**, 771–781.
 - 26 Sadeh A, Movshovich N, Volokh M, Gheber L and Aharoni A (2011) Fine-tuning of the Msn2/4-mediated yeast stress responses as revealed by systematic deletion of Msn2/4 partners. *Mol Biol Cell* **22**, 3127–3138.
 - 27 Elfving N, Chereji RV, Bharatula V, Björklund S, Morozov AV and Broach JR (2014) A dynamic interplay of nucleosome and Msn2 binding regulates kinetics of gene activation and repression following stress. *Nucleic Acids Res* **42**, 5468–5482.
 - 28 Berry DB and Gasch AP (2008) Stress-activated genomic expression changes serve a preparative role for impending stress in yeast. *Mol Biol Cell* **19**, 4580–4587.
 - 29 Treger JM, Schmitt AP, Simon JR and McEntee K (1998) Transcriptional factor mutations reveal regulatory complexities of heat shock and newly identified stress genes in *Saccharomyces cerevisiae*. *J Biol Chem* **273**, 26875–26879.
 - 30 Haruki H, Nishikawa J and Laemmli UK (2008) The anchor-away technique: rapid, conditional establishment of yeast mutant phenotypes. *Mol Cell* **31**, 925–932.
 - 31 Janke C, Magiera MM, Rathfelder N, Taxis C, Reber S, Maekawa H, Moreno-Borchart A, Doenges G, Schwob E, Schiebel E *et al.* (2004) A versatile toolbox for PCR-based tagging of yeast genes: new fluorescent proteins, more markers and promoter substitution cassettes. *Yeast* **21**, 947–962.
 - 32 Liesche J, Marek M and Günther-Pomorski T (2015) Cell wall staining with trypan blue enables quantitative analysis of morphological changes in yeast cells. *Front Microbiol* **6**, 107.
 - 33 Kucsera J, Yarita K and Takeo K (2000) Simple detection method for distinguishing dead and living yeast colonies. *J Microbiol Methods* **41**, 19–21.
 - 34 Collart MA and Oliviero S (1993) Preparation of yeast RNA. *Curr Protoc Mol Biol* **23**, 13.12.1–13.12.5.
 - 35 Wallace EWJ, Kear-Scott JL, Pilipenko EV, Schwartz MH, Laskowski PR, Rojek AE, Katanski CD, Riback JA, Dion MF, Franks AM *et al.* (2015) Reversible, specific, active aggregates of endogenous proteins assemble upon heat stress. *Cell* **162**, 1286–1298.
 - 36 Wessel D and Flugge UI (1984) A method for the quantitative recovery of protein in dilute solution in the presence of detergents and lipids. *Anal Biochem* **138**, 141–143.
 - 37 Rappsilber J, Mann M and Ishihama Y (2007) Protocol for micro-purification, enrichment, pre-fractionation and storage of peptides for proteomics using StageTips. *Nat Protoc* **2**, 1896–1906.
 - 38 Cox J, Hein MY, Lubner CA, Paron I, Nagaraj N and Mann M (2014) Accurate proteome-wide label-free quantification by delayed normalization and maximal peptide ratio extraction, termed MaxLFQ. *Mol Cell Proteomics* **13**, 2513–2526.
 - 39 Cox J and Mann M (2008) MaxQuant enables high peptide identification rates, individualized p.p.b.-range mass accuracies and proteome-wide protein quantification. *Nat Biotechnol* **26**, 1367–1372.
 - 40 Tyanova S, Temu T, Sinitcyn P, Carlson A, Hein MY, Geiger T, Mann M and Cox J (2016) The Perseus computational platform for comprehensive analysis of (prote)omics data. *Nat Methods* **13**, 731–740.

- 41 Benjamini Y and Hochberg Y (1995) Controlling the false discovery rate: a practical and powerful approach to multiple testing. *J R Stat Soc Series B Stat Methodology* **57**, 289–300.
- 42 Howe KL, Contreras-Moreira B, De Silva N, Maslen G, Akanni W, Allen J, Alvarez-Jarreta J, Barba M, Bolser DM, Cambell L *et al.* (2020) Ensembl genomes 2020—enabling non-vertebrate genomic research. *Nucleic Acids Res* **48**, D689–D695.
- 43 Bonfert T, Kirner E, Csaba G, Zimmer R and Friedel CC (2015) ContextMap 2: fast and accurate context-based RNA-seq mapping. *BMC Bioinformatics* **16**, 122.
- 44 Liao Y, Smyth GK and Shi W (2014) featureCounts: an efficient general purpose program for assigning sequence reads to genomic features. *Bioinformatics* **30**, 923–930.
- 45 Anders S and Huber W (2010) Differential expression analysis for sequence count data. *Genome Biol* **11**, R106.
- 46 Hotelling H (1933) Analysis of a complex of statistical variables into principal components. *J Educ Psychol* **24**, 417–441.
- 47 Pedregosa F, Varoquaux G, Gramfort A, Michel V, Thirion B, Grisel O, Blondel M, Prettenhofer P, Weiss R and Dubourg V (2011) Scikit-learn: machine learning in python. *J Mach Learn Res* **12**, 2825–2830.
- 48 PlotlyTechnologiesInc (2015) Collaborative data science.
- 49 Capaldi AP, Kaplan T, Liu Y, Habib N, Regev A, Friedman N and O’Shea EK (2008) Structure and function of a transcriptional network activated by the MAPK Hog1. *Nat Genet* **40**, 1300–1306.
- 50 Coleman ST, Fang TK, Rovinsky SA, Turano FJ and Moye-Rowley WS (2001) Expression of a glutamate decarboxylase homologue is required for normal oxidative stress tolerance in *Saccharomyces cerevisiae*. *J Biol Chem* **276**, 244–250.
- 51 Caspeta L, Chen Y and Nielsen J (2016) Thermotolerant yeasts selected by adaptive evolution express heat stress response at 30 °C. *Sci Rep* **6**, 27003.
- 52 Anderson RM, Bitterman KJ, Wood JG, Medvedik O and Sinclair DA (2003) Nicotinamide and PNC1 govern lifespan extension by calorie restriction in *Saccharomyces cerevisiae*. *Nature* **423**, 181–185.
- 53 Santhanam A, Hartley A, Düvel K, Broach JR and Garrett S (2004) PP2A phosphatase activity is required for stress and tor kinase regulation of yeast stress response factor Msn2p. *Eukaryot Cell* **3**, 1261–1271.
- 54 Finley D, Ozkaynak E and Varshavsky A (1987) The yeast polyubiquitin gene is essential for resistance to high temperatures, starvation, and other stresses. *Cell* **48**, 1035–1046.
- 55 Jolliffe IT and Cadima J (2016) Principal component analysis: a review and recent developments. *Philos Trans A Math Phys Eng Sci* **374**, 20150202.
- 56 Jain NK and Roy I (2009) Effect of trehalose on protein structure. *Protein Sci* **18**, 24–36.
- 57 Causton HC, Ren B, Koh SS, Harbison CT, Kanin E, Jennings EG, Lee TI, True HL, Lander ES and Young RA (2001) Remodeling of yeast genome expression in response to environmental changes. *Mol Biol Cell* **12**, 323–337.
- 58 Chen RE and Thorner J (2007) Function and regulation in MAPK signaling pathways: lessons learned from the yeast *Saccharomyces cerevisiae*. *Biochim Biophys Acta* **1773**, 1311–1340.
- 59 Mogk A, Bukau B and Kampinga HH (2018) Cellular handling of protein aggregates by disaggregation machines. *Mol Cell* **69**, 214–226.
- 60 Mogk A, Ruger-Herreros C and Bukau B (2019) Cellular functions and mechanisms of action of small heat shock proteins. *Annu Rev Microbiol* **73**, 89–110.
- 61 Haslbeck M, Walke S, Stromer T, Ehrnsperger M, White HE, Chen SX, Saibil HR and Buchner J (1999) Hsp26: a temperature-regulated chaperone. *EMBO J* **18**, 6744–6751.
- 62 Haslbeck M, Braun N, Stromer T, Richter B, Model N, Weinkauff S and Buchner J (2004) Hsp42 is the general small heat shock protein in the cytosol of. *EMBO J* **23**, 638–649.
- 63 Specht S, Miller SBM, Mogk A and Bukau B (2011) Hsp42 is required for sequestration of protein aggregates into deposition sites in. *J Cell Biol* **195**, 617–629.
- 64 Ungelenk S, Moayed F, Ho CT, Grousl T, Scharf A, Mashaghi A, Tans S, Mayer MP, Mogk A and Bukau B (2016) Small heat shock proteins sequester misfolding proteins in near-native conformation for cellular protection and efficient refolding. *Nat Commun* **7**, 13673.
- 65 Mühlhofer M, Peters C, Kriehuber T, Kreuzeder M, Kazman P, Rodina N, Reif B, Haslbeck M, Weinkauff S and Buchner J (2021) Phosphorylation activates the yeast small heat shock protein Hsp26 by weakening domain contacts in the oligomer ensemble. *Nat Commun* **12**, 6697.
- 66 Xie Y and Varshavsky A (2001) RPN4 is a ligand, substrate, and transcriptional regulator of the 26S proteasome: a negative feedback circuit. *Proc Natl Acad Sci U S A* **98**, 3056–3061.
- 67 Samanta MP and Liang S (2003) Predicting protein functions from redundancies in large-scale protein interaction networks. *Proc Natl Acad Sci U S A* **100**, 12579–12583.
- 68 Cherry PD, Peach SE and Hesselberth JR (2019) Multiple decay events target HAC1 mRNA during splicing to regulate the unfolded protein response. *Elife* **8**, e42262.
- 69 UniprotDB (2021) UniProt: the universal protein knowledgebase in 2021. *Nucleic Acids Res* **49**, D480–D489.
- 70 Rosenzweig AC (2002) Metallochaperones: bind and deliver. *Chem Biol* **9**, 673–677.
- 71 Schwanhold N, Iobbi-Nivol C, Lehmann A and Leimkühler S (2018) Same but different: comparison of

- two system-specific molecular chaperones for the maturation of formate dehydrogenases. *PLoS ONE* **13**, e0201935.
- 72 Stuehr DJ and Haque MM (2019) Nitric oxide synthase enzymology in the 20 years after the Nobel prize. *Br J Pharmacol* **176**, 177–188.
- 73 Macossay-Castillo M, Marvelli G, Guharoy M, Jain A, Kihara D, Tompa P and Wodak SJ (2019) The balancing act of intrinsically disordered proteins: enabling functional diversity while minimizing promiscuity. *J Mol Biol* **431**, 1650–1670.
- 74 Luo H, Lin Y, Gao F, Zhang CT and Zhang R (2014) DEG 10, an update of the database of essential genes that includes both protein-coding genes and noncoding genomic elements. *Nucleic Acids Res* **42**, D574–D580.
- 75 Voellmy R, Boellmann F. Chaperone Regulation of the Heat Shock Protein Response. In: Csermely P, Vigh L, editors. *Molecular Aspects of the Stress Response: Chaperones, Membranes and Networks*. Advances in Experimental Medicine and Biology, vol 594. New York, NY: Springer; 2007. https://doi.org/10.1007/978-0-387-39975-1_9
- 76 Masser AE, Kang W, Roy J, Mohanakrishnan Kaimal J, Quintana-Cordero J, Friedländer MR and Andréasson C (2019) Cytoplasmic protein misfolding titrates Hsp70 to activate nuclear Hsf1. *Elife* **8**, e47791.
- 77 Truman AW, Kristjansdottir K, Wolfgeher D, Ricco N, Mayampurath A, Volchenboum SL, Clotet J and Kron SJ (2015) The quantitative changes in the yeast Hsp70 and Hsp90 interactomes upon DNA damage. *Data Brief* **2**, 12–15.
- 78 Kolhe JA, Babu NL and Freeman BC (2023) The Hsp90 molecular chaperone governs client proteins by targeting intrinsically disordered regions. *Mol Cell* **83**, 2035–2044.e7.
- 79 Kuang Z, Pinglay S, Ji H and Boeke JD (2017) Msn2/4 regulate expression of glycolytic enzymes and control transition from quiescence to growth. *Elife* **6**, e29938.
- 80 Amorós M and Estruch F (2001) Hsf1p and Msn2/4p cooperate in the expression of *Saccharomyces cerevisiae* genes HSP26 and HSP104 in a gene- and stress type-dependent manner. *Mol Microbiol* **39**, 1523–1532.
- 81 Pincus D, Anandhakumar J, Thiru P, Guertin MJ, Erkin AM and Gross DS (2018) Genetic and epigenetic determinants establish a continuum of Hsf1 occupancy and activity across the yeast genome. *Mol Biol Cell* **29**, 3168–3182.
- 82 Sanz AB, García R, Rodríguez-Peña JM and Arroyo J (2017) The CWI pathway: regulation of the transcriptional adaptive response to Cell Wall stress in yeast. *J Fungi (Basel)* **4**, 1.
- 83 Rodríguez-Peña JM, García R, Nombela C and Arroyo J (2010) The high-osmolarity glycerol (HOG) and cell wall integrity (CWI) signalling pathways interplay: a yeast dialogue between MAPK routes. *Yeast* **27**, 495–502.
- 84 Hinnebusch AG (2005) Translational regulation of GCN4 and the general amino acid control of yeast. *Annu Rev Microbiol* **59**, 407–450.
- 85 Crawford RA and Pavitt GD (2019) Translational regulation in response to stress in *Saccharomyces cerevisiae*. *Yeast* **36**, 5–21.
- 86 Cappelletti V, Hauser T, Piazza I, Pepelnjak M, Malinowska L, Fuhrer T, Li Y, Dörig C, Boersema P, Gillet L *et al.* (2021) Dynamic 3D proteomes reveal protein functional alterations at high resolution in situ. *Cell* **184**, 545–559.e22.
- 87 Jarzab A, Kurzawa N, Hopf T, Moerch M, Zecha J, Lejten N, Bian Y, Musiol E, Maschberger M and Stoehr G (2020) Meltome atlas—thermal proteome stability across the tree of life. *Nat Methods* **17**, 495–503.
- 88 Tsuboyama K, Osaki T, Matsuura-Suzuki E, Kozuka-Hata H, Okada Y, Oyama M, Ikeuchi Y, Iwasaki S and Tomari Y (2020) A widespread family of heat-resistant obscure (hero) proteins protect against protein instability and aggregation. *PLoS Biol* **18**, e3000632.
- 89 Vecchi G, Sormanni P, Mannini B, Vandelli A, Tartaglia GG, Dobson CM, Hartl FU and Vendruscolo M (2020) Proteome-wide observation of the phenomenon of life on the edge of solubility. *Proc Natl Acad Sci U S A* **117**, 1015–1020.
- 90 Noji M, Samejima T, Yamaguchi K, So M, Yuzu K, Chatani E, Akazawa-Ogawa Y, Hagihara Y, Kawata Y, Ikenaka K *et al.* (2021) Breakdown of supersaturation barrier links protein folding to amyloid formation. *Commun Biol* **4**, 120.
- 91 Kuge S, Jones N and Nomoto A (1997) Regulation of yAP-1 nuclear localization in response to oxidative stress. *EMBO J* **16**, 1710–1720.
- 92 Perez-Riverol Y, Csordas A, Bai J, Bernal-Llinares M, Hewapathirana S, Kundu DJ, Inuganti A, Griss J, Mayer G, Eisenacher M *et al.* (2019) The PRIDE database and related tools and resources in 2019: improving support for quantification data. *Nucleic Acids Res* **47**, D442–D450.
- 93 Edgar R, Domrachev M and Lash AE (2002) Gene expression omnibus: NCBI gene expression and hybridization array data repository. *Nucleic Acids Res* **30**, 207–210.
- 94 Ashburner M, Ball CA, Blake JA, Botstein D, Butler H, Cherry JM, Davis AP, Dolinski K, Dwight SS, Eppig JT *et al.* (2000) Gene ontology: tool for the unification of biology. The Gene Ontology Consortium. *Nat Genet* **25**, 25–29.
- 95 Kanehisa M and Goto S (2000) KEGG: kyoto encyclopedia of genes and genomes. *Nucleic Acids Res* **28**, 27–30.
- 96 Eden E, Navon R, Steinfeld I, Lipson D and Yakhini Z (2009) GOrilla: a tool for discovery and visualization of enriched GO terms in ranked gene lists. *BMC Bioinformatics* **10**, 48.

Supporting information

Additional supporting information may be found online in the Supporting Information section at the end of the article.

Fig. S1. Cells without Hsf1 are only arrested not dead.

Fig. S2. Cells lacking Hsf1 do not adapt to mild heat stress within 30 min.

Fig. S3. Sporulation is the main upregulated process in the strain without all three TFs.

Fig. S4. Protein aggregation correlates with stress severity.